Regulation of human endothelial nitric oxide synthase mRNA stability through sterol-responsive elements: multiple cis-acting elements and trans-acting factors

Guo Hua Song

The Graduate School

Yonsei University

Department of Medicine

Regulation of human endothelial nitric oxide synthase mRNA stability through sterol-responsive elements: multiple cis-acting elements and trans-acting factors

A Dissertation

Submitted to the Department of Medicine

and the Graduate School of Yonsei University

in partial fulfillment of the

requirements for the degree of

Doctor of Medicine

Guo Hua Song

July 2008

This certifies that the dissertation
of Guo Hua Song is approved.

_____

Thesis Supervisor : Jae Won Choi, M.D., Ph.D.

_____

Committee Member : In Hong Choi, M.D., Ph.D.

_____

Committee Member : Yung Chien Teng, M.D., Ph.D.

_____

Committee Member : Joo Young Park, M.D., Ph.D.

_____

Committee Member : Jang Young Kim, M.D., Ph.D.

The Graduate School

Yonsei University

July 2008

ACKNOWLEDGEMENTS

First and foremost, I would like to express gratitude to my supervisor Dr. Jae Won Choi who gave me a great opportunity to challenge the degree of Ph.D. During the past four years, he has advised me with his integral view on research, frequent encouragement, and generous support throughout this work. Without his help, this work would not be possible. I owe him lots of gratitude for having me shown this way of research. I would also like to express my sincere gratitude to the members of my dissertation committee, Drs. In Hong Choi, Yung Chien Teng, Joo Young Park and Jang Young Kim for their invaluable advice and patience. Their readiness to help me is also appreciated. In particular, I gratefully thank Dr. Yung Chien Teng for his concerns in life and encouragement during my four years Ph.D. training.

I would like to thank the members of Pharmacology Department for their discussion, concerns and supports. Very special thanks are expressed to Dr. Sung Wan Ahn and Assistant Hee Jeong Kim for their supports in Korean languages. I am also indebted to my Chinese friends who have been or are studying in this college.

Finally, I feel a deep sense of gratitude to my parents, for the support and love they have shown me with throughout these years, in good times and difficult times. They have given me the strength and courage to mount greater heights and pursue my dreams, wherever they may be.

CONTENTS

LIST OF TABLES

LIST OF FIGURES

ABSTRACT

Regulation of human endothelial nitric oxide synthase mRNA stability through sterol-responsive elements: multiple cis-acting elements and trans-acting factors

Guo Hua Song

Dept. of Medicine

The Graduate School

Yonsei University

Statins lower serum cholesterol by inhibiting the rate-limiting enzyme in the mevalonate pathway of cholesterol synthesis. So it is often used as pharmaceutical agents in people with or at risk of cardiovascular disease. There are many reports showing that statins exhibit action beyond lipid-lowering activity in the prevention of atherosclerosis. Previously, we have reported that lovastatin increased the levels of eNOS mRNA at a post-transcriptional level using HUVEC (human umbilical vein endothelial cell)-derived cell line, EA.hy926. Lovastatin stabilized eNOS mRNA by depriving intracellular sterols, including mevalonate or geranylgeranyl pyrophosphate (GGPP). Because GGPP was required for the isoprenylation of various intracellular signaling molecules, such effect of lovastatin seemed to be mediated by intracellular signaling pathways. In this experiment, either hydroxyfasudil, a Rho-kinase inhibitor, or cytochalasin D, a disrupter of the actin cytoskeleton, upregulated the levels of eNOS mRNA. These data indicated that the status of cellular architecture regulated by

Rho-mediated pathways may play a role in determining the decay rate of eNOS mRNA. We also proved that 3´-untranslated regions (3´UTR) and the adjacent coding regions of eNOS mRNA harbored the cis-acting elements necessary to regulate eNOS mRNA decays. In this experiment, we aimed to determine the precise sequences and the exact locations of these cis-acting elements. Several mutants corresponding to CU-rich elements were prepared. Data from transfection experiments showed that six elements, UCCUC, UUCUC, CUUU, UCCUU, CCUCC and CCUCU were functional in the regulation of eNOS mRNA stability. In order to verify the presence of trans-acting factors associated with these cis-acting elements, RNA-protein binding assay using radiolabelled RNA probes was performed and an approximate 60 kDa ribonucleoprotein (RNP) complex was detected. The binding activity of this RNP complex was increased in the presence of lovastatin. In order to determine the identity of this RNA-binding protein, UV-crosslinking studies using biotin-labelled RNA probes and two dimensional gel electrophoresis were performed. Analysis of Maldi-TOF spectrum identified β-actin protein as the major component of this RNP complex. These data indicated that binding of β-actin protein to CU-rich elements played a functional role in the regulation of eNOS mRNA stability. Our results provided a basis for future studies on the mechanisms of regulation of transcripts stability.

Key words: Statin, eNOS mRNA stability, CU-rich elements, 60 kDa ribonucleoprotein, β-actin

Ⅰ. Introduction

1.1. Characteristics and functions of nitric oxide synthase

Nitric oxide synthase (NOS) produces nitric oxide (NO) by catalysing a five-electron oxidation of a guanidino nitrogen of L-arginine (L-Arg) to L-citrulline[1]. Three different forms of NOS have been classified : an endothelial isoform (eNOS), which is localized in the endothelium under physiological conditions, generates NO in blood vessels and is involved with regulating vascular function; an inducible isoenzyme (iNOS), which requires cytokines or endotoxin activation for its expression and can be found in the immune system but is also found in the cardiovascular system[1, 2]. And the neuronal NOS (nNOS), which produces NO in neuronal tissue and performs a role in intercellular communication.

Endothelium–derived NO is an important mediator of vasodilation in response to a wide variety of stimuli, and plays a critical role in both the regulation of endothelial function and the control of blood pressure. Release of NO in response to shear-stress or stimulation with agonists such as bradykinin and acetylcholine is responsible for the moment-to-moment adjustment of vascular diameter, and maintenance of optimal conductance characteristics of the arterial tree[3-5]. Endothelial NO is not only a potent vasodilator, but it can inhibit leukocyte–endothelial adhesion, vascular smooth muscle migration and proliferation, and platelet aggregation, all of which are important steps in atherogenesis[5]. Thus, the dysregulation of NO synthesis in the endothelium may have far ranging influences in vascular pathophysiology and may lead to vascular disorders, including atherosclerosis.

1.2. Regulation of eNOS gene expression

1.2.1. Regulation of eNOS gene expression

The eNOS is described as a ‘constitutive’ NOS in endothelial cells and the levels of eNOS were initially thought to be static. It had been generally accepted that the eNOS activity is primarily regulated by calmodulin and $[Ca^{2+}]_i$. However, recent research revealed new mechanisms controlling eNOS activity with multiple additional regulatory steps[6], including gene transcription, mRNA stability, posttranslational modification (phosphorylation, myristoylation, palmitoylation), and intracellular localization (membrane bound versus cytoplasmic, interaction with caveolae). In cultured endothelial cells, transforming growth factor-β1, oxidized linoleic acid, 3-hydroxy-3-methylglutaryl coenzyme A (HMG-CoA) reductase inhibitors, cell growth, lysophosphatidylcholine, shear stress, and hydrogen peroxide have been shown to increase eNOS gene expression. However, hypoxia, lipopolysaccaride, thrombin, oxidized LDL and tumor necrosis factor-α can decrease eNOS mRNA levels[2, 7-10]. For many of these stimuli, both transcriptional and posttranscriptional mechanisms contribute to the regulation of eNOS gene expression.

1.2.1.1. Transcriptional regulation: eNOS promotor and cis-regulatory elements

The eNOS gene encodes a mRNA of approximate 4,000 nucleotides (nt) and is present as a single copy in the haploid human genome. The eNOS promoter has been cloned from many species and there is a high degree of sequence homology among different species[11]. Sequence analysis of 5'-flanking regions revealed multiple potential cis-regulatory DNA sequences in the setting of a ‘TATA-less’ promoter, including a CCTA box, Sp1 sites, GATA motifs, CACCC boxes, AP-1 and AP-2 sites, a P53 binding region, NF-1 element, shear-stress response elements, acute phase reactant regulatory elements, and sterol-regulatory elements[12].

Early work have described that trans-acting factors Sp1 and GATA-2 bind to proximal promoter elements and mediate the basal transcription of eNOS gene in quiescent systemic endothelium[12, 13]. However, the mechanism of basal transcription of eNOS remained poorly characterized until the identification of two tightly clustered cis-positive regulatory elements in the proximal core promoter of the human eNOS gene. Positive regulatory domain I (PRD I; -104 to -95 relative to the transcription initiation site) was found to bind Sp1 and two variants of Sp3[14]. The other regulatory region, positive regulatory domain II (PRD II; -144 to -115) encompasses a 30-bp region of the core promoter and binds transcription factors Ets-1, Elf-1, YY1, Sp1, and MYC-associated zinc finger protein[14]. Furthermore, functional interactions between these trans-acting factors that bind to these two regulatory domains seems to be critical for eNOS promoter activation. Mutating cis-elements in PRD I or PRD II disrupted cooperative activation of the human promoter[14]. Positive and negative protein–protein and protein–DNA interactions were identified over a 50-bp region of the core human eNOS promoter. These data highlight the complex nature of the eNOS promoter and the fact that its regulation involves multiple cis and trans interactions.

Chromatin-based mechanisms and epigenetic events also regulate the expression of eNOS gene at the transcriptional level in a cell-restricted fashion. It has been reported that eNOS promoter was more heavily methylated in nonendothelial cells than in endothelial cells by using methylation-sensitive isoschizomer mapping and high-resolution sodium bisulfite genomic sequencing. Methylation of eNOS promoter-reporter regions was associated with a marked impairment of promoter activity in mammalian cells[15]. DNA methylation of promoters is often accompanied by histone modifications that render the chromatin effectively inaccessible to transcription factors [16-18]. Taking all evidence into account, DNA methylation and chromatin structure regulate the endothelial cells-specific conformation of eNOS promoter.

1.2.1.2. Posttranscriptional regulation: the regulation of eNOS mRNA stability

Most of signals regulate eNOS mRNA levels, at least in part, by modulating eNOS mRNA stability. For example, Laufs et al observed HMG-CoA reductase inhibitors attenuated the ability of hypoxia to destabilize eNOS mRNA in human saphenous vein endothelial cells[19]. In addition, Yoshizumi et al reported that addition of tumor necrosis factor-α (TNF-α) to human umbilical vein endothelial cells decreased eNOS mRNA level by decreasing the stability of the mRNA [10]. Furthermore, Bouloumie et al showed that vascular endothelial growth factor increases endothelial eNOS mRNA stability[20].

The balance between gene transcription and mRNA degradation shows steady-state mRNA levels. The half-lives of mRNA in mammalian cells may vary over a wide range (from minutes to many hours) and can be regulated by extracellular and/or intracellular signals. The mechanisms regulating mRNA stability are multiple and diverse although it is less clear than that regulating gene transcription. It is well-known that mRNA can be stabilized by posttranscriptional modifications including a 7-methylguanosine cap structure at the 5` end and a poly(A) tail at the 3` end[21, 22]. Moreover, ongoing translation has an important role in the regulation of mRNA stability via the stabilization by inhibitors of translation elongation[21, 22]. On the other hand, premature and aberrant translation termination, as well as impaired translation initiation, can promote mRNA degradation[21, 22].

The regulation of mRNA stability has emerged as a critical control step in determining cellular mRNA levels. Searles et al[23] aimed at understanding the molecular mechanisms for the regulation of eNOS mRNA stability in response to changes in the endothelial cell proliferative state. They examined the decrease in eNOS mRNA levels in cultured bovine aortic endothelial cells (BAECs) in transition from a proliferative to a postconfluent state. There was no difference in the transcriptional rate of eNOS in proliferating and postconfluent BAECs, whereas eNOS mRNA stability was

markedly increased in proliferating cells. They hypothesized that mRNA-binding proteins may have an important role in the modulation of eNOS mRNA stability, UV cross linking RNA-protein binding experiments were done, then cis-acting RNA sequences were found and a cytoplasmic protein that bound to those “destabilizing” sequences were characterized. Alonso have reported that cytosolic proteins of bovine endothelial cells formed complexes with in vitro transcribed 3`UTR of eNOS mRNA[24]. The binding activity of these cytosolic proteins was enhanced by cytokines which are commonly found in atherosclerotic lesions i.e. TNF-α, and was correlated with higher eNOS mRNA destabilization[24, 25]. Some researchers also demonstrated that cerivastatin prevented the downregulation of eNOS protein expression by TNF-α. They also shown that cerivastatin inhibits the binding activity of TNF-α - induced endothelial cytosolic proteins to 3`UTR of eNOS mRNA and is associated with eNOS mRNA stabilization[26].

The rate of mRNA degradation is controlled, at least in part, by nucleotide sequences, which are typically located in the 3`UTR or coding region of the mRNA. These “cis-acting” nucleotide sequences may just be sequence specific for the binding of trans-acting proteins, or they may form secondary stem-loop RNA structures that facilitate binding of regulatory “trans-acting” proteins.

It seems that cis-acting sequences and corresponding RNA-binding proteins varied differentially in response to different mRNA-stabilizing/destabilizing signals[23, 24, 27]. Analysis of sequence homology between human and bovine eNOS 3`UTR reveals an unexpectedly high degree of sequence homology in the 3`UTR (approximately 66% of 430 nt in the bovine 3`UTR are identical to those in the human sequence)[28], suggesting that the cis-acting sequences in the 3`UTR, which are functional in the regulation of eNOS mRNA stability, have been conserved during evolution.

1.2.2. Regulation of eNOS gene expression by statins

Statins upregulate the expression of eNOS via a to-date undefined mechanism, although it is well-known to occur by stabilization of eNOS mRNA[29-31]. Lovastatin is an inhibitor of HMG-CoA reductase, an enzyme which catalyzes the conversion of HMG-CoA to mevalonate. Mevalonate is a required building block for cholesterol biosynthesis and lovastatin interferes with its production by acting as a competitive inhibitor for HMG-CoA which binds to the HMG-CoA reductase. Therefore, statins are frequently prescribed to prevent coronary heart disease. Large clinical trials have shown that the inhibition of cholesterol biosynthesis by HMG-CoA reductase inhibitors or statins improves clinical outcomes in patients with atherosclerosis [32, 33]. Although this protective effect of statins seems to be the direct result of its cholesterol-lowering properties, statins also exert various beneficial pleiotropic effects in those with cardiovascular diseases[34-36]. The cholesterol-independent or "pleiotropic" effects of statins include the upregulation and activation of eNOS. Because statins inhibit an early step in the cholesterol biosynthetic pathway, they also inhibit the synthesis of isoprenoids such as farnesylpyrophosphate and geranylgeranyl pyrophosphate, which are required for posttranslational modification of intracellular signaling molecules such as Rho GTPases. The regulation of eNOS levels by Rho GTPases, therefore, may be an important mechanism underlying the cardiovascular protective effect of statins[37]. Because intracellular factors regulating this phenomenon have remained elusive, we decided to investigate the underlying regulatory mechanisms in human umbilical vein endothelial cell (HUVEC) - derived cell line, EA.hy926.

Previously, we had reported the effects of lovastatin on the expression of eNOS gene at the posttranscriptional level. After treatment of 25 uM of lovastatin, eNOS mRNA levels reached submaximal levels at 12 hours and reached plateau at 24 hours. In the presence of 5,6-dichloro-1-β-D-ribofuranosylbenzimidazole, a transcription inhibitor, or cycloheximide, a translation inhibitor, such effects of lovastatin were blocked.

Among sterols examined in our experiments, geraniol or farnesyl pyrophosphate could not block the effect of lovastatin, however, mevalonate or geranylgeranyl pyrophosphate completely blocked the effects of lovastatin and significantly decreased eNOS mRNA half-life. In order to determine whether cis-acting elements are necessary for the regulation of eNOS mRNA stability, four different chimeric gene constructs which contain a part of the human eNOS cDNA were prepared using pEGFP-C2/stop1.2. The data from transfection experiments shows the existence of cis-acting elements in heNOS_D fragment which contains the 3`UTR and the adjacent coding regions of eNOS cDNA.

The aim of the present study was to determine and characterize the molecular mechanisms controlling eNOS mRNA stability. As the data showed that 3`UTR and the adjacent coding regions have paramount importance in the regulation of the stability of eNOS mRNA, we specifically examined RNA-protein interactions at this region and analyzed whether or not statin modify the binding activity of the cytosolic proteins, then tried to identify the trans-factor binding protein through mass spectrum technics.

Ⅱ. Materials & Methods

2.1. Cell culture

EA.hy926 cells were maintained in Dulbecco's Modified Eagle Medium (Gibco, Auckland, N.Z.) containing 10% fetal bovine serum (FBS), 2 mM L-glutamine, 100 units/ml penicillin, and 10 μg/ml streptomycin. For experimental purposes, cells were cultured in a medium containing 10% delipidized FBS (DFBS) and 25 μM lovastatin. DFBS was prepared as described by Choi et al. (1998): 50 ml of FBS was added to 500 ml of prechilled 1 : 1 mixture of ethanol (Merck, Darmstadt, Germany) : acetone (Sigma Chemical Co, St. Louis, MO, USA) and stirred for 4 hrs to precipitate proteins. Then samples were filtered through #1 Whatman filter 1001 - 125 paper (Whatman, Maidstone, England) using a Buchner and vacuum. After liquid passed through the filter paper, 100 ml of ethyl ether (Sigma Chemical Co, St. Louis, MO, USA) was added directly onto the paper and let the paper dry at room temperature. Proteins were then scrapped from paper into a beaker and let it overnight with a cover at 4°C. The next day, proteins were transferred to a lyophilizer beaker (ILSHIN lab, Gyeonggi-Do, South Korea) and dissolved in 100 ml of distilled water, after which proteins were lyophilized for two days and dissolved in 100 ml distilled water, sterilized by passing through the filter of 0.2 μm pore size in the hood and then stored at -80°C until use. EA.hy926 cells were kindly provided by Dr. Edgell (Department of Pathology, University of North Carolina at Chapel Hill). Lovastatin was provided by Choong Wae Pharmaceuticals (Seoul, South Korea) and was prepared as described by Kita et al. (1980): 40 mg of lovastatin sodium powder was dissolved in 0.9 ml of pre-warmed ethanol (55°C) and 0.45 ml of 0.6 N sodium hydroxide was added followed by adding 7 ml of distilled water. Mixture was then incubated at room temperature for 30 min and pH was adjusted to 8.0 by using hydrochloric acid. Total volume was adjusted to 9.3 ml with distilled water to make a final concentration of 10 mM. After filtration through a filter of 0.22

µm pore size, lovastatin solution was aliquoted and stored at -80°C until use.

2.2. RNA isolation

A single step method of RNA isolation using acid guanidinium/thiocyanate/ phenol/chloroform extraction was used throughout this study[38]. After removing culture medium, EA.hy926 cells grown in monolayer were washed twice with PBS. One ml of solution D (4 M guanidinium thiocyanate, 25 mM sodium citrate, pH 7.0, 0.5% N-laurosylsarcosine and 0.1 M 2-mercaptoethanol) was added directly to a 60 mm culture dish and cells were collected by using cell scraper to a polypropylene tube. Then the following was added sequentially to 1 ml of lysate: 0.1 ml of 2 M sodium acetate, pH 4.0, mix thoroughly by inversion; 1 ml water-saturated phenol solution, pH 4.3 ± 0.2 (Sigma Chemical Co, St. Louis, MO, USA), mix thoroughly by inversion; 0.2 ml of chloroform/isoamyl alcohol (49:1), vortex vigorously for 10 s. After that, samples were cooled on ice for 15 min and then centrifuged for 20 min (13,000 rpm, 4°C). The upper aqueous phase, which contained mostly RNA, was transferred carefully to a clean tube. One ml of isopropanol was added to precipitate the RNA and then samples were kept at -20°C for at least 2 hrs. Following centrifugation for 20 min (13,000 rpm, 4°C), a gel-like RNA pellet was dissolved in 0.3 ml of solution D and transferred to a 1.5-ml microcentrifuge tube. Then 0.3 ml of isopropanol was added and samples were incubated for at least 1 hr at -20 °C. After centrifugation for 10 min (13,000 rpm, 4 °C), RNA pellet was washed twice with 80% ethanol and dissolved in 30 - 50 µl of DEPC-treated water. Afterwards, RNA samples were incubated for 5 min at 75 °C and then quickly chilled on ice to ensure complete solubilization and denature the secondary structure. RNA quantity and purity were measured by using spectrophotometric readings at wavelengths of 260 nm and 280 nm. Then the RNA samples were diluted by DEPC-water to the concentration of 200 ng/µl and immediately used for further experiments or kept at -80°C until use.

2.3. Reverse transcription (RT)

cDNA synthesis was performed using 600 ng of total RNA, 25 mM $MgCl_2$ solution 4 µl, 10×PCR buffer 2 µl, 2.5 mM each dNTP mixture 8 µl, 1 unit/µl RNase inhibitor 1 µl, 2.5 unit/µl MuLV Reverse Transcriptase 1 µl, and 50 µM oligo $d(T)_{16}$ primer 1 µl. Total reaction volume, including sample, was 20 µl. RT reaction was extended at 42°C for 45 min, denatured at 95°C for 5 min, and then cooled at 5°C for 5 min. The reagents for reverse transcription were all from Applied Biosystems (Foster City, CA, USA).

2.4. Real-time PCR

The primers used for real-time PCR are listed in Table 1. PCR samples were amplified using a SYBR-green PCR 2 × master mix kit (QIAGEN GmbH, Hilden, Germany) and a Rotor-Gene 2000 (Corbett Research, Sydney, Australia). In some cases, real-time PCR was also performed in the same condition by using Power SYBR-green PCR 2 × master mix (Applied Biosystems, Foster City, CA,USA) and a ABI PRISM 7700 system (Applied Biosystems, Foster City, CA,USA). PCR reactions were run in 20 µl of reaction mixtures containing 10 µl of SYBR-green PCR 2 × master mix, 2µl of cDNA sample, 1.7 µl of 1 pmol/µl forward primer, 1.7 µl of 1 pmol/µl reverse primer, 4.6 µl of nuclease-free distilled water by using the conditions listed in Table 2: 95℃ for 15 min followed by 40 cycles of amplification step. During each cycle, DNA strands were melted for 15 sec at 94°C and then extended for 60 sec at 60°C. And then melting curve analysis step was performed by increasing temperatures gradually from 60°C to 99°C in 5 min. The data was analyzed by using Rotor-gene software ver. 6.0 (Corbett Research, Sydney, Australia) or ABI sequence detection system 1.9.1 (Applied Biosystems, Foster City, CA, USA). Relative mRNA levels were calculated as $2^{\Delta\Delta Ct}$. $\Delta\Delta Ct = \Delta E - \Delta C$. $\Delta E = Ct_{sample} - Ct_{GAPDH}$. $\Delta C = Ct_{control} - Ct_{GAPDH}$. The levels of target

mRNAs relative to GAPDH mRNA were determined. Data was expressed as means +/- S.E.M. and differences between groups were considered significant for *P* values < 0.05.

Table 1. Real time PCR primers

Primer	Accession #	Sequence	Predicted size
GFP	U57606	F ACACCCTGGTGAACCGCAT R CCATGATATAGACGTTGTGGCTGTT	111 bp
heNOS	NM_000603	F CTCATGGGCACGGTGATG R ACCACGTCATACTCCCATACAC	152 bp
GAPDH	NM_002046	F AACAGCGACACCCATCCTC R CATACCAGGAAATGAGCTTGACAA	85 bp

F : forward, R : reverse

Table 2. Real time PCR conditions

Step	Temperature (°C)	Time	Cycle number
Initial Activation	95	15 min	1
Amplification (Cycling)	94 60	15 sec 60 sec	40
Melting curve	60~99	5 min	1

2.5. Transfection of chimeric gene constructs

DNA construct plasmids used for transfection experiment were prepared by QIAGEN plasmid mini kit for purification of transfection grade plasmid (QIAGEN GmbH, Hilden, Germany) as described in the manual provided with the manufacturer. Then the DNA concentrations were accurately determined using 260-nm absorption following the estimation of DNA content based on the intensity of agarose gel bands. The DNA purities were also determined using a A260nm/A280nm ratio. Only the DNA plasmids whose ratios were between 1.8~2.0 were used for the further experiments.

Transient transfection was performed by using FuGENE 6 reagent (Roche diagnostic, Indianapolis, USA) as described by the manufacturer. For initial optimization experiments, EA.hy926 cells approximate 70 – 80% confluent were transfected in a 24-well culture plate, using 3:2, 3:1, and 6:1 ratios of FuGENE 6 (µl) to DNA construct (µg), respectively. The experiment was performed in duplicate, group 1 and 2. The volume of FuGENE 6 and the mass of DNA used for optimization experiment are listed in Table 3. FuGENE 6 reagent was pipetted directly into Opti - MEM serum free medium (Life Technologies, Grand Island, NY, USA) without allowing contact with the walls of plastic tubes and incubated for 5 min at room temperature. Then DNA constructs were added to the diluted FuGENE 6. The complexes were mixed well and incubated for 20 min at room temperature, after which the complexes were added in a drop-wise manner to the cells grown in one 24-well culture plate with 0.5 ml of normal medium per well. 24 hrs after transfection, the cells were observed directly under a Fluorescence Microscope Model IX51 (Olympus Corporation, Tokyo, Japan). Total viable cell numbers and GFP-positive cell numbers were counted in three random areas, named 1, 2, and 3, of each well (shown in Table 3). Also, total cell numbers including dead cells which were suspended and floated in the medium in those areas were counted. And then, transfection efficiencies were determined by calculating the ratios of cell numbers between GFP positive cells and total cells. Cell viabilities were determined using a ratio between viable cell numbers and total cell numbers. As shown in Table 3, combination of 0.6 µl FuGENE 6 and 0.4 µg DNA gave the highest transfection efficiency of approximate 40.57% and a low

death rate of approximate 5%. Therefore, this ratio between the volume of FuGENE 6 and the mass of DNA was determined to be used in the following transfection experiments. As the 100-mm cell culture dishes need to be used in the further experiments, the starting volume of FuGENE 6 and the starting mass of DNA were adjusted to 18 µl and 12 µg in proportion to the relative surface areas of 24 well-1 well (1.9 cm^2)/100 mm dish (55 cm^2). Transfection experiments in 100-mm dishes were performed as described in Table 3 following the procedure described above. After confirming transfection efficiencies and cell viabilities 24 hrs post-transfection, the cells were divided into four or five 60-mm cell culture dishes. Addition of drugs to medium was performed until cells became stable (approximate 24hr after division). Total RNAs were prepared 48 hrs after drug treatment.

Table 3. Optimization experiment in a 24-well culture plate and transfection experiment in a 100-mm culture dish using FuGENE 6 reagent

	Container	Surface area (cm2)	Typical total volume of medium (ml)	Tube label	Opti-MEM medium (µl)	FuGENE 6 reagent (µl)	DNA (µg)	Group	Area	Total cell numbers	GFP-positive cell numbers	Total viable cell numbers	Cell viability (%)	Cell viability mean (%)	Transfection efficiency (%)	Transfection efficiency mean (%)
O	24 well-1 well	1.9	0.5	1(3:1)	19.4	0.6	0.2	1	1	440	43	440	100	100	9.77272727	10.369787
									2	300	30	300	100		10	
									3	380	39	380	100		10.2631579	
								2	1	367	47	367	100		12.8065395	
									2	312	36	312	100		11.5384615	
									3	370	29	370	100		7.83783784	
				2(3:2)	19.4	0.6	0.4	1	1	264	101	240	90.909	94.9	38.2575758	40.57337
									2	302	128	298	98.675		42.384106	
									3	262	110	250	95.42		41.9847328	
								2	1	289	112	269	93.08		38.7543253	
									2	345	156	331	95.942		45.2173913	
									3	304	112	290	95.395		36.8421053	
				3(6:1)	18.8	1.2	0.2	1	1	280	60	270	96.429	94.869	21.4285714	20.602244
									2	366	48	345	94.262		13.1147541	
									3	276	76	261	94.565		27.5362319	
								2	1	298	63	278	93.289		21.1409396	
									2	254	48	239	94.094		18.8976378	
									3	321	69	310	96.573		21.4953271	
				4(3:2)	18.8	1.2	0.4	1	1	240	60	220	91.667	90.95	25	29.95202
									2	200	76	184	92		38	
									3	256	66	228	89.063		25.78125	
								2	1	298	90	271	90.94		30.2013423	
									2	295	77	263	89.153		26.1016949	
									3	309	107	287	92.88		34.6278317	
T	100 mm	55	10	T(3:2)	582	18	12	1	1	323	118	315	97.523	95.351	36.5325077	40.619187
									2	307	115	293	95.44		37.4592834	
									3	344	168	331	96.221		48.8372093	
								2	1	337	123	317	94.065		36.4985163	
									2	318	134	299	94.025		42.1383648	
									3	329	139	312	94.833		42.2492401	

O: optimization experiment; T: transfection experiment

2.6. Construction of chimeric gene constructs

1) Plasmids for transfection experiments: A certain part of eNOS cDNA was inserted into the EcoRI and BamHI restriction enzyme sites located in the multiple cloning site (MCS) of pEGFP-C2/stop1.2 vector (Clontech, Palo Alto, CA, USA). The restriction map and MCS of pEGFP-C2/stop1.2 vector was shown in Figure 1. This vector contains two stop codons: the first one locates between GFP coding region and MCS, the second one locates at the end of MCS. The sequences of the cDNA fragments inserted into the vector are depicted in Figure 2. cDNA fragments were made by PCRs which were performed in a reaction volume of 50 µl containing primers (0.8 µmol each), 50 ng template of eNOPuc13 plasmid, 1.25 unit Taq DNA polymerase(Applied Biosystems, Foster City, CA,USA), 1.5 mmol $MgCl_2$ (Applied Biosystems, Foster City, CA,USA), and 0.2 mmol dNTPs(Applied Biosystems, Foster City, CA,USA). Primers designed to contain EcoRI or BamHI restriction enzyme sites at 5'-flanking regions are listed in Table 4. The sequences underlined indicate the additional EcoRI and BamHI recognition sites and sequences in boldface indicate the corresponding flanking bases for enzyme to bind and cleave efficiently. PCR reactions were run in a condition as shown in Table 5: 94°C for 2 min, then 30 cycles of 94°C for 1 min followed by the annealing temperatures, which were different among heNOS_D fragments, for 1 min followed by 1 min of extension at 72°C. Agarose gel electrophoresis was run and target bands were excised. QIAquick gel extraction kit (QIAGEN GmbH, Hilden, Germany) was used to extract PCR products from agarose gels according to the protocols supplied by manufacturer. Then the products were digested by EcoRI and BamHI enzymes (Promega, Madison, WI, USA), after which agarose gel was run and target cDNA inserts were extracted by using QIAquick gel extraction kit. pEGFP-C2/stop1.2 vector which was used for ligation experiment was also prepared by EcoRI and BamHI digestion in the same way. Ligation was carried out by using a DNA Ligation Kit ver.2.1 (TaKaRa Bio Inc, Otsu, Shiga, Japan) in a 10 µl of reaction volume containing 5 µl of

TaKaRa ligation solution I, 100 ng of lineared pEGFP-C2/stop1.2 vector, cDNA insert (8:1 of molar ratio of insert:vector), and TE buffer, pH 8.0. Following incubating the reaction at 16°C for overnight, ligation products were transformed into chemically competent *E. coli*, JM 109 cells, and grown overnight on LB-kanamycin plates at 37°C. Colonies were screened for the presence of the appropriately sized plasmid using the "colony crack" method (Maniatis et al., Molecular Cloning: A Laboratory Manual, Cold Springs Harbor Literature, pp. 270-247, 1982.): pEGFP-C2/stop1.2 vectors containing inserts of foreign DNA were distinguished from the parent plasmids based on their size as estimated by electrophoresis in agarose gels following "colony cracks" to release the plasmid DNA from transformants. Then, DNA miniprep purification kit (Promega, Madison, WI, USA) was used to extract construct DNA plasmids from the screened colonies. The base sequence identity of all plasmid constructs were verified by restriction enzyme digestion and/or DNA sequencing which was performed by Macrogen Inc. (Seoul, Korea).

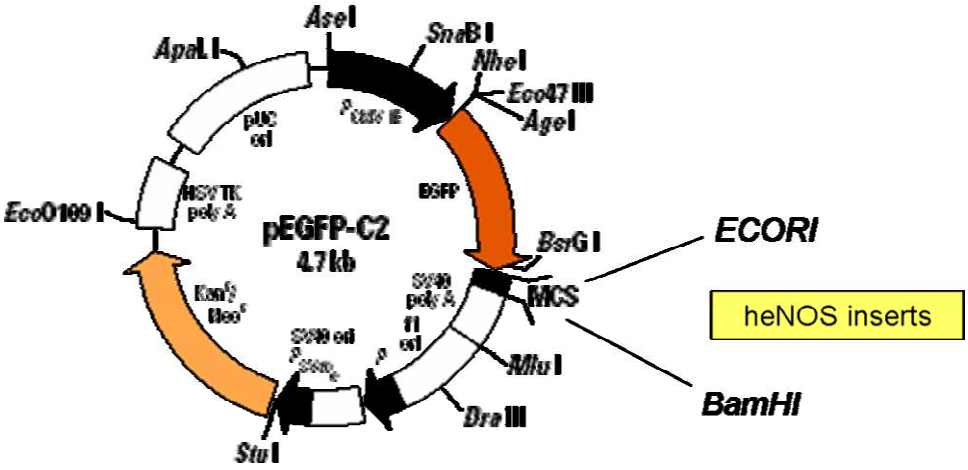

Fig. 1. Restriction Map and Multiple Cloning Sites (MCS) of pEGFP-C2/stop1, 2.

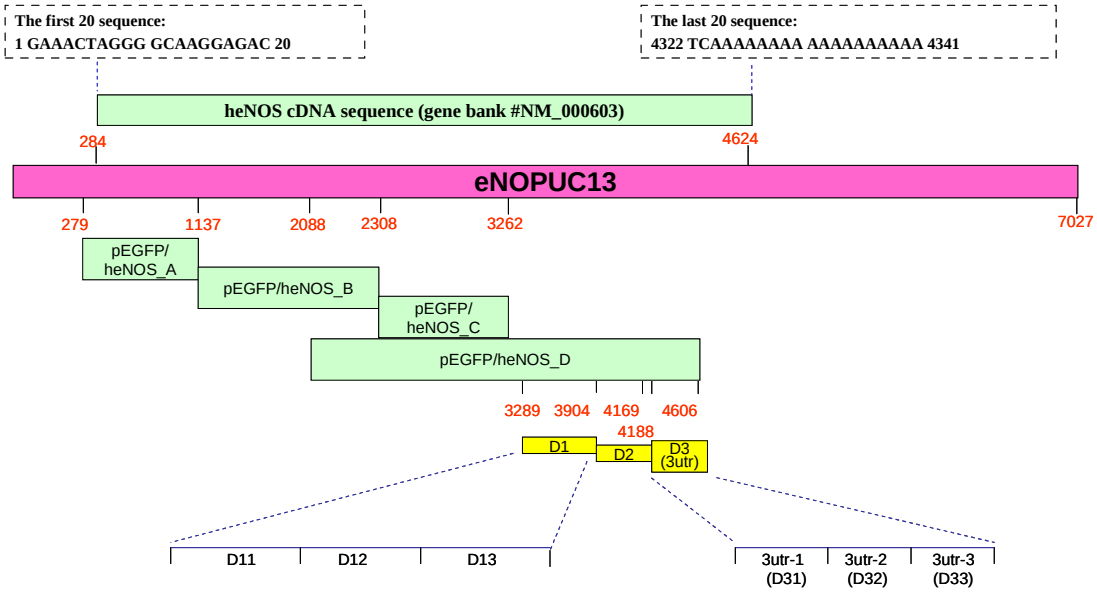

Fig. 2. Construction of chimeric DNA

Table 4. Primer pairs used for making heNOS fragments

Primer	Sequence	Predicted size
D1	F **CG**GAATTC**CG**CGACGCTACG R **CG**GGATCC**CG**AAACATGTGGC	645 bp
D2	F **CG**GAATTC**CG**GGGGCCACAT R **CG**GGATCC**CG**GGGGCTGTTG	287 bp
3UTR	F **CG**GAATTC**CG**TCAGACACCAA R **CG**GGATCC**CG**GAGCTGGGGT	439 bp
D1-1	F **CG**GAATTC**CG**CGACGCTACG R **CG**GGATCC**CG**CCCAGCCCAT	234 bp
D1-2	F **CG**GAATTC**CG**CACTATGGAG R **CG**GGATCC**CG**GGTAGAGATG	279 bp
D1-3	F **CG**GAATTC**CG**GCGACGAGGT R **CG**GGATCC**CG**AAACATGTGGC	184 bp
3UTR-1	F **CG**GAATTC**CG**CCCTGAGAGC R **CG**GGATCC**CG**GAATCCTTGC	158 bp
3UTR-2	F **CG**GAATTC**CG**GGATTCAGCA R **CG**GGATCC**CG**TTCGACTAAG	174 bp
3UTR-3	F **CG**GAATTC**CG**CGAATGTTAGA R **CG**GGATCC**CG**GAGCTGGGGT	162 bp

F : forward, R : reverse; GAATTC : EcoRI site, GGATCC : BamHI site

Table 5. PCR conditions used for making heNOS fragments

Step		Temperature (°C)		Time	Cycle number
Initial Activation		94		2 min	1
Amplification (Cycling)	**Denaturation**	94		1 min	30
	Annealing	D1	57	1 min	
		D2	59		
		3UTR	55		
		D1-1	60		
		D1-2	51		
		D1-3	59		
		3UTR-1	57		
		3UTR-2	55		
		3UTR-3	56		
	Extension	72		1 min	
Extension		72		7 min	1

2) Plasmids for in vitro transcription experiments: Seven parts of eNOS cDNA (D11, D12, D13, D2, 3utr-1, 3utr-2, and 3utr-3) were ligated into pGEM-3Z vector (Promega, Madison, WI, USA) at the EcoRI and BamHI sites according to the same principle with step 1. pGEM-3Z vector contains T7 promotor sequence just at 5` end ahead of EcoRI site as shown in Figure 3. LB-ampicillin plates were used for screening pGEM-3Z transformants. The base sequence identities of all plasmid constructs were also verified by restriction enzyme digestion and/or DNA sequencing.

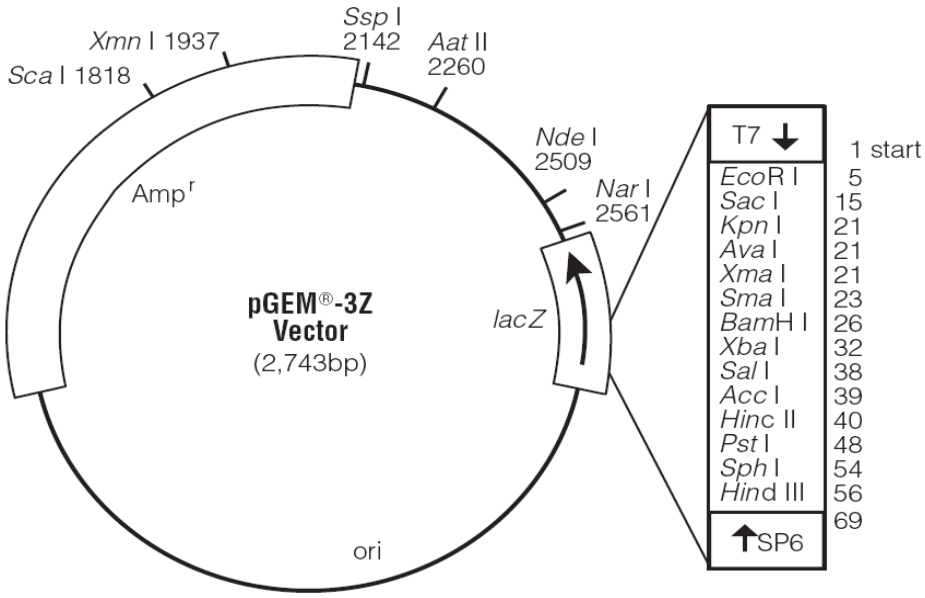

Fig. 3. pGEM-3Z Vector circle map and sequence reference points

2.7. Site-directed mutagenesis for in vitro transcription and transfection experiments

The sequences of cDNA fragments are shown below. The sequences in boldface indicate the multiple CU-rich regions. And sequences in highlight indicates the possible

cis-elements reported previously[28, 39]. One report has shown that a 39-kDa ribonucleoprotein complex failed to form after substituting CAAGC for CCTCC motif[39], indicating CAAGC represents an unfunctional sequence. Therefore, in our experiment, site-directed mutants were made by substituting CAAGC for the possible cis-elements which contain five nucleotides, and substituting CAAG/AAGC for cis-elements which contains 4 nucleotides. A ‘megaprimer’ PCR method[40] was used to make some of these mutants. This method was based on the design of forward and reverse flanking primers with significantly different melting temperatures (T_m). Primers were listed below. A mega primer was synthesized in the first PCR reaction using a mutagenic primer, the low T_m flanking primer and a low annealing temperature. The second PCR reaction was performed in the same tube as the first PCR and utilized the high T_m flanking primer, the megaprimer product of the first PCR and a high annealing temperature, which prevented priming by the low T_m primer from the first PCR reaction.

1) D1-3 sequence

CGGAATTCCGGCGACGAGGTGCAGAACGCCCAGCAGCGCGGGGTGTTTGGCCGAG**TCC TCACCGCCTTCTCCC**GGGAACCTGACAACCCCAAGACCTACGTGCAGGACATCCTGAG GACGGAGCTGGCTGCGGAGGTGCACCGCGTGCTGTGCCTCGAGCGGGGCCACATGTTTC GGGATCCCG

Three mutants, namely by D1-3 mutant 1, D1-3 mutant 2, D1-3 mutant 3, were made according to D1-3 sequence. D1-3 mutant 1 was synthesized by substituting CAAGC for TCCTC, the first cis-element. The ‘megaprimer’ PCR method for making mutant 1 was outlined in Figure 4: the two flanking primers of D1-3 mutant 1 were different in length. The short, `reverse' flanking primer was just 15 bases long and typically had a calculated $T_m$ of 45°C. The long, `forward' flanking primer was designed to be 29 bases long and had a calculated T_m of 79°C. The first PCR reaction was carried out using the short flanking primer, the internal mutagenic primer and a low annealing temperature of 44°C. Then, the second, high T_m flanking primer was added directly to

the reaction tube. The second step PCR was performed using a high annealing temperature of 72°C. The high annealing temperature assured that the final PCR product can be generated through selective priming by the megaprimer product of the first PCR and the high T_m flanking primer. The short flanking primer that remained from the first PCR did not interfere with the second PCR synthesis because of its poor efficiency of annealing to the template at 72°C.

The first PCR amplifications were performed in 100 µl reaction mixtures containing 0.5 µl Taq polymerase, 200 pg D1-3 wild-type template, 200 µM of dNTPs in the 1 × PCR buffer. All the PCR reagents were supplied by Applied Biosystems (Foster City, CA, USA). 10 pmol of D1-3 mutant 1 mutagenic primer and 100 pmol of D1-3 mutant 1 short flanking primer were employed for 25 cycles of amplification using the conditions shown in Table 6. After completion of the first PCR, 0.5 µl Taq polymerase and 3µl containing 7.5 nmol of each dNTP were added to the reaction tube, which was mixed gently and spun briefly. The second PCR was then initiated asymmetrically by subjecting the reaction mixture to five cycles of 94°C for 40 s and 72°C for 90 s. Following the five asymmetric cycles utilizing only the megaprimer, which may improve the efficiency of the megaprimer amplification step, 100 pmol of D1-3 mutant 1 long flanking primer was added, and the reaction was continued for 25 cycles with the same two-step temperature profile as shown in Table 6.

D1-3 mutant 2 was synthesized by substituting CAAGC for TTCTC, the second cis-element, according to the same principle and PCR condition with mutant 1.

D1-3 mutant 3 was made by substituting CAAGC for both TCCTC and TTCTC. Mutant 1 was used as template for synthesizing mutant 3 in the same PCR condition. Primers are listed in Table 7.

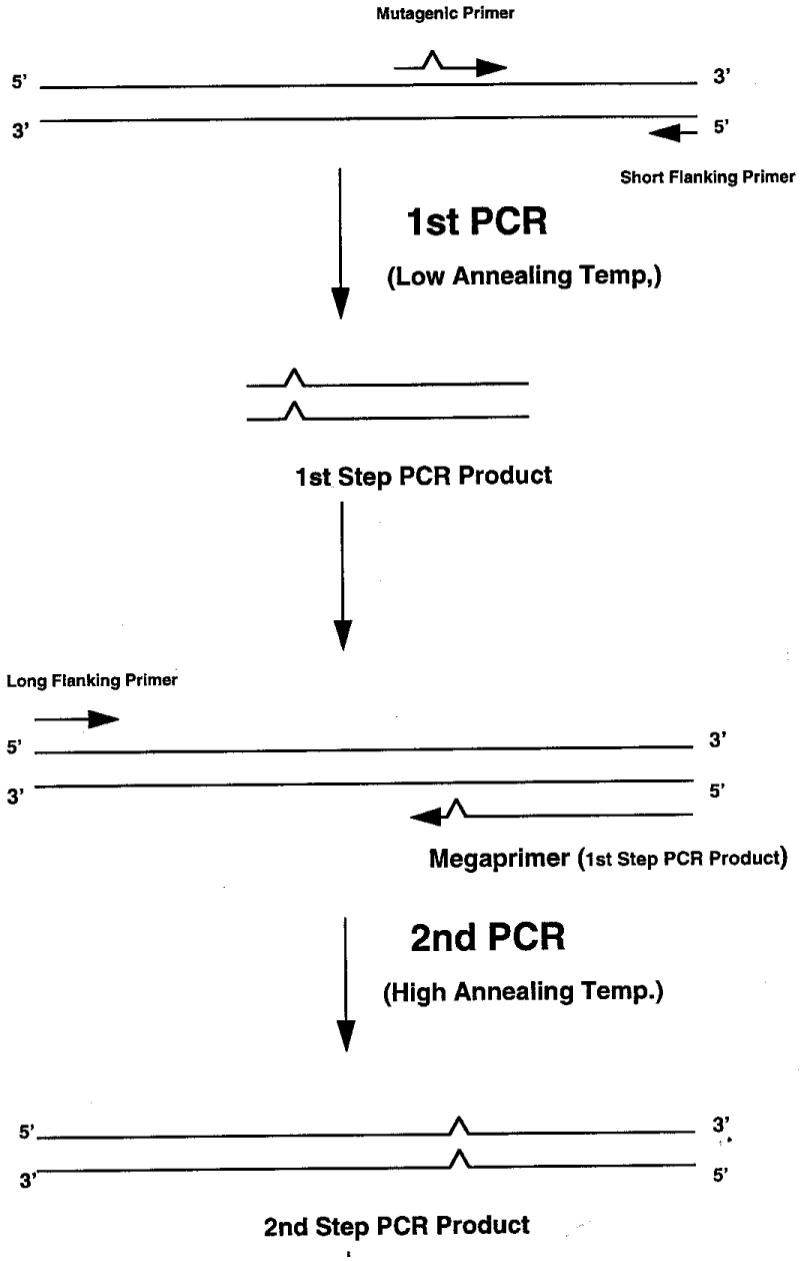

Fig. 4. Schematic outline of the 'megaprimer' PCR mutagenesis protocol used in this study

Table 6. PCR conditions used for making D1-3 mutants

Step			Temperature (°C)	Time	Cycle number
1st PCR	Initial Activation		94	4 min	1
	Amplification (Cycling)	Denaturation	94	40 sec	25
		Annealing	44	1 min	
		Extension	72	40 sec	
	Extension		72	5 min	1
2nd PCR	Denaturation		94	40 sec	5
	Annealing & Extension		72	90 sec	
	Adding 100 pmol of D1-3 mutant 1 long flanking primer				
	Denaturation		94	40 sec	25
	Annealing & Extension		72	90 sec	

Table 7. Primer pairs used for making D1-3 mutants

Primer	Sequence
D1-3 mutant1	M AGCAAGCACCGCCTTCTC
	S CGGGATCCCGAAACA
	L CGGAATTCCGGCGACGAGGTGCAGAACGC
D1-3 mutant2	M TCCTCACCGCCCAAGCC
	S CGGGATCCCGAAACA
	L CGGAATTCCGGCGACGAGGTGCAGAACGC
D1-3 mutant3	M CAAGCACCGCCCAAGCC
	S CGGGATCCCGAAACA
	L CGGAATTCCGGCGACGAGGTGCAGAACGC

M : mutagenic primer, S : short flanking primer, L : long flanking primer

CAAGC : mutated sequence

2) D2 sequence

CGGAATTCCGGGGGCCACATGTTTGTCTGCGGCGATGTTACCATGGCAACCAACGTCCTG
CAGACCGTGCAGCGCATCCTGGCGACGGAGGGCGACATGGAGCTGGACGAGGCCGGCG
ACGTCATCGGCGTGCTGCGGGATCAGCAACGCTACCACGAAGACATTTTCGGGCTCACG
CTGCGCACCCAGGAGGTGACAAGCCGCATACGCA**CCCAGAGCTTTTCCTT**GCAGGAGC
GTCAGTTGCGGGGCGCAGTGCCCTGGGCGTTCGACCCTCCCGGCTCAGACACCAACAGC
CCCTCGGGATCCCG

Three mutants corresponding to D2 were made. D2 mutant 1 was synthesized by substituting CAAGC for TCCTT and D2 mutant 2 was synthesized by substituting AAGC for CTTT. D2 mutant 3 was made by substituting both of them. PCR principles and conditions were totally same with that for D1-3 mutants. Primers are listed in Table 8.

Table 8. Primer pairs used for making D2 mutants

Primer		Sequence
D2 mutant1	M	CTTTCAAGCGCAGGAGC
	S	CGGGATCCCGAGGG
	L	CGGAATTCCGGGGGCCACATGTTTGTCTGC
D2 mutant2	M	AAGCTCCTTGCAGGAGCG
	S	CGGGATCCCGAGGG
	L	CGGAATTCCGGGGGCCACATGTTTGTCTGC
D2 mutant3	M	AAGCCAAGCGCAGGAGC
	S	CGGGATCCCGAGGG
	L	CGGAATTCCGGGGGCCACATGTTTGTCTGC

M : mutagenic primer, S : short flanking primer, L : long flanking primer

CAAGC, AAGC : mutated sequence

3) 3UTR-1 sequence

CGGAATTCCGCCCTGAGAGCCG**CCTGG**CTTT**CCCTTCC**AGTTCCGGGAGAGCGGCTGC
CCGACTCAGGTCCGCCCGACCAGGATCAG**CCCCGCT**CCTCCCCTCTTTGAGGTGGTGCC
TTCTCACATCTGTCCAGAGGCTGCAAGGATTCCGGGATCCCG

Five mutants corresponding to 3UTR-1 were made. 3UTR-1 mutant 1 was synthesized by substituting CAAG for CTTT, the first cis-element. The PCR method for making 3UTR-1 mutant 1 was outlined in Figure 5: the mutagenesis site was located at the proximal 5` end of 3UTR-1 sequence. Therefore, one-step PCR was carried out using the proximal mutagenic primer, the flanking primer, and an appropriate annealing temperature designed according to the T_m of two primers. PCR amplifications were performed in 100 µl reaction mixtures containing 0.5 µl Taq polymerase, 200 pg 3UTR-1 wild-type template, 200 µM of dNTPs, 100 pmol of 3UTR-1 mutant 1 mutagenic primer, 100 pmol of 3UTR-1 mutant 1 flanking primer in the 1 × PCR buffer. Twenty-five cycles of amplification was performed using the reaction conditions shown in Table 9.

Mutant 2 and 3 were synthesized by substituting CAAGC for CCTCC and CCTCT, respectively. Mutant 4 was made by substituting CAAGC for both CCTCC and CCTCT. PCR amplifications for making mutant 2, 3 and 4 were performed in the same principle and conditions with that for D1-3 mutant 1 using the ‘megaprimer’ PCR method. 3UTR-1 mutant 3 was the template for making mutant 4.

Mutant 5 was synthesized by mutating all of the three cis-elements. PCR was run in the same principle and condition with that of 3UTR-1 mutant 1 by one-step PCR method using 3UTR-1 mutant 4 as template. Primers are listed in Table 10.

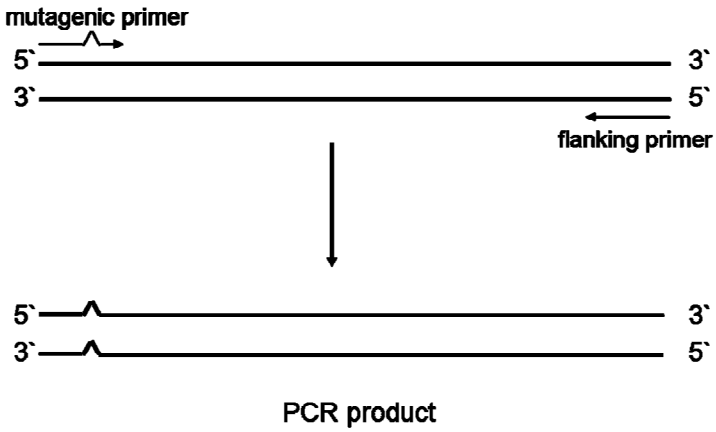

Fig. 5. Schematic outline of the one-step PCR mutagenesis protocol used in this study

Table 9. PCR conditions used for making 3UTR-1 mutant 1

Step		Temperature (°C)	Time	Cycle number
Initial Activation		94	4 min	1
Amplification (Cycling)	Denaturation	94	40 sec	25
	Annealing & Extension	72	100 sec	
Extension		72	5 min	1

Table 10. Primer pairs used for making 3UTR-1 mutants

Primer		Sequence
3UTR-1 mutant1	M	CGGAATTCCGCCCTGAGAGCCGCCTGGCAAGC
	F	CGGGATCCCGGAATCCTTGCAGCCTCTGGACAG
3UTR-1 mutant2	M	CGCTCAAGCCCTCTTGAG
	S	CGGGATCCCGGAATC
	L	CGGAATTCCGCCCTGAGAGCCGCCTGG
3UTR-1 mutant3	M	CGCTCCTCCCAAGCTGAG
	S	CGGGATCCCGGAATC
	L	CGGAATTCCGCCCTGAGAGCCGCCTGG
3UTR-1 mutant4	M	CGCTCAAGCCAAGCTGAG
	S	CGGGATCCCGGAATC
	L	CGGAATTCCGCCCTGAGAGCCGCCTGG
3UTR-1 mutant5	M	CGGAATTCCGCCCTGAGAGCCGCCTGGCAAGC
	F	CGGGATCCCGGAATCCTTGCAGCCTCTGGACAG

M : mutagenic primer; F : flanking primer; S : short flanking primer; L : long flanking primer; CAAGC, CAAG : mutated sequence

4) 3UTR-2 sequence

CGGAATTCCGGGATTCAGCATTATTGCTCCAGGAAGGAGCAAAACG**CCTCTTTTCCCTC**
TCTAGGCCTGTTGCCTCGGGCCTGGGTCCGCCTTAATCTGGAAGG**CCCCTCC**CAGCAGC
GGTACCCCAGGGCCTACTGCCACCCGCTTCCTGTTTCTTAGTCGAACGGGATCCCG

Five mutants corresponding to 3UTR-2 were made. 3UTR-2 mutant 1, 2 and 3 was synthesized by substituting CAAGC for CCTCT, CCTCT, CCTCC, respectively. 3UTR-2 mutant 4 was made by substituting CAAGC for both of the first two cis-elements, CCTCT and CCTCT, using mutant 2 as template. And, 3UTR-2 mutant 5

was made by mutating all of the three cis-elements with mutant 4 as template. PCR methods for making 3UTR-2 mutants were performed in the same principles and conditions with that of D1-3 mutant 1 by the 'megaprimer' method. Primers are listed in Table 11.

Table 11. Primer pairs used for making 3UTR-2 mutants

Primer		Sequence
3UTR-2 mutant1	M	AACGCAAGCTTTCCCTCT
	S	CGGGATCCCGTTCG
	L	CGGAATTCCGGGATTCAGCATTATTCCTCC
3UTR-2 mutant2	M	AACGCCTCTTTTCCAAGC
	S	CGGGATCCCGTTCG
	L	CGGAATTCCGGGATTCAGCATTATTCCTCC
3UTR-2 mutant3	M	CCAAGCCAGCAGCGGTAC
	S	CGGGATCCCGTTCG
	L	CGGAATTCCGGGATTCAGCATTATTCCTCC
3UTR-2 mutant4	M	AACGCAAGCTTTCCAAGC
	S	CGGGATCCCGTTCG
	L	CGGAATTCCGGGATTCAGCATTATTCCTCC
3UTR-2 mutant5	M	CCAAGCCAGCAGCGGTAC
	S	CGGGATCCCGTTCG
	L	CGGAATTCCGGGATTCAGCATTATTCCTCC

M : mutagenic primer; S : short flanking primer; L : long flanking primer;

CAAGC : mutated sequence

5) 3UTR-3 sequence

CGGAATTCCGCGAATGTTAGA**TT**CCTCT**TG**CCTCT**CTC**AGGAGTATCTTACCTGTAAAG
TCTAATCTCTAAATCAAGTATTTATTATTGAAGATTTACCATAAGGGACTGTGCCAGATGTT
AGGAGAACTACTAAAGTGCCTACCCCAGCTCCGGGATCCCG

Three mutants corresponding to 3UTR-3 were made. 3UTR-3 mutant 1 and 2 were synthesized by substituting CAAGC for 1st and 2nd CCTCT, respectively. 3UTR-3 mutant 3 was made by substituting CAAGC for both of the two cis-elements. Mutant 2 was used as template for synthesizing mutant 3. PCR principles and conditions for 3UTR-3 mutants were totally same with that for 3UTR-1 mutant 1 using one-step PCR method. Primers are listed in Table 12.

Sequence comparison of CU-rich elements among wild-type and mutants of all five cDNA fragments was summarized in Table 13.

All the PCR products were verified by agarose gel electrophoresis, and then ligated into pEGFP-C2/stop1.2 or pGEM-3Z vector as described above. All the mutated constructs were also sequenced to confirm the absence of the expected mutations.

Table 12. Primer pairs used for making 3UTR-3 mutants

Primer		Sequence
3UTR-3 mutant1	M	CGGAATTCCGCGAATGTTAGATTCAAGCTGCCTCT
	F	CGGGATCCCGGAGCTGGGGTAGGC
3UTR-3 mutant2	M	CGGAATTCCGCGAATGTTAGATTCCTCTTGCAAGCCTC
	F	CGGGATCCCGGAGCTGGGGTAGGC
3UTR-3 mutant3	M	CGGAATTCCGCGAATGTTAGATTCAAGCTGCAAGCCTC
	F	CGGGATCCCGGAGCTGGGGTAGGC

M : mutagenic primer; F : flanking primer; CAAGC : mutated sequence

Table 13. Sequence comparison of cis-elements among wild-type and mutants of all cDNA fragments

CU-rich elements	D13	D2	3UTR-1	3UTR-2	3UTR-3
W	TCCTC…TTCTC	CTTTTCCTT	CTTT…CCTCCCCTCT	CCTCTTTTCCCTCT…CCTCC	CCTCTTGCCTCT
M 1	CAAGC…TTCTC	CTTTCAAGC	CAAG…CCTCCCCTCT	CAAGCTTTCCCTCT…CCTCC	CAAGCTGCCTCT
M 2	TCCTC…CAAGC	AAGCTCCTT	CTTT…CAAGCCCTCT	CCTCTTTTCCAAGC…CCTCC	CCTCTTGCAAGC
M 3	CAAGC...CAAGC	AAGCCAAGC	CTTT…CCTCCCAAGC	CCTCTTTTCCCTCT…CAAGC	CAAGCTGCAAGC
M 4			CTTT…CAAGCCAAGC	CAAGCTTTCCAAGC…CCTCC	
M 5			CAAG…CAAGCCAAGC	CAAGCTTTCCAAGC…CAAGC	

W: wild-type, M 1: mutant 1, M 2 : mutant 2, M 3 : mutant 3, M 4 : mutant 4, M 5 : mutant 5

2.8. In vitro transcription

All the pGEM-3Z constructs were linearized by BamHI digestion prior to being used as templates for in vitro transcription, except that one more template (heNOS_D21) was generated by restriction digestion of pGEM-3Z/D2 plasmid with NaeI. Therefore, D21 RNA probe contains the 5` end part of heNOS_D2 sequence. Radioisotope-labelled RNAs were synthesized by using T7 riboprobe system (Promega, Madison, WI, USA) in a 20 µl reaction volume containing 4 µl of transcription optimized 5 × buffer, 2 µl of 100 mM DTT, 1 µl of 40 units/µl RNA inhibitor, 4 µl of rATP, rGTP, rUTP mix (2.5 mM ea), 2.4 µl of 100µM rCTP, 1 µg of linearized template DNA, 1 µl of 20 units/µl T7 RNA polymerase, and 50 µCi of [^{32}P-α]CTP (Perkin Elmer life sciences, Woodbridge, ON, Canada). Biotinylated RNAs were synthesized by using MAXIscript T7 kit (Ambion, Austin, TEX, USA) in a 20 µl reaction volume containing 2 µl of 10 × transcription buffer, 1 µl of 10 mM rATP, 1 µl of 10 mM rGTP, 1 µl of 10 mM rCTP, 0.6 µl of 10 mM rUTP, 1µg of linearized template DNA, 2 µl of T7 enzyme mix, and 0.4 µl of 10 mM biotin-16-UTP (Roche diagnostic, Indianapolis, USA). After transcription at 37°C for 1 hour, RNase-Free DNase (2 U/µl) was added to the reaction mixture to digest DNA templates, and the transcribed RNAs were purified by passing through Sephadex G-50 columns (Roche diagnostic, Indianapolis, USA) for radioisotope labeled probes or NucAway™ Spin Columns (Ambion, Austin, TEX, USA) for biotinylated probes to remove unincorporated ribonucleotides according to the supplier's protocol. Specific activities of radioisotope labeled probes were measured by using scintillation cocktail. The quantities of biotinylated probe were measured by using spectrophotometric readings at wavelengths of 260 nm and 280 nm.

2.9. Preparation of cellular extracts

EA.hy926 cells were cultured as previously described. Cytoplasmic extracts were prepared according to the protocol by Patrick F.H. Lai et al [28]. Cells at proliferous time were washed three times in PBS and then harvested by using cell scraper in PBS. Following centrifugation at 1,850 g (10 min, 4°C), cell pellets were resuspended in a hypotonic lysis buffer consisting of 10 mM HEPES (pH 7.9), 40 mM KCl, 3 mM $MgCl_2$, 1 mM DTT, 5% glycerol, 0.2% Nonidet P-40, 1 μg/ml aprotinin, 0.5 μg/ml leupeptin, and 0.5 mM phenylmethylsulfonylfluoride (all from Sigma Chemical Co, St. Louis, MO, USA). After incubating on ice for 1 hr, samples were mechanically homogenized with Dounce homogenizer (10 strokes) on ice. The nuclei and debris were removed by centrifugation (14,000 rpm, 15 min, 4°C), and the cytoplasmic fraction (supernatant) were aliquoted and immediately used for the next step or frozen at −80°C until use. Protein concentrations were determined by Bradford method (Bio-Rad, Hercules, CA, USA).

2.10. Ultra-violet (UV) irradiation cross-linking studies

RNAs used in UV-cross linking assays were heated at 85°C for 5 min, then kept at room temperature for 20 min, and reannealed at hybridization temperature (30°C) for 3.5 hours to restore the secondary structure and binding affinity[41-43]. Fifteen μg of EA.hy926 cell lysate was mixed with 300-500 ng of total yeast RNA in a reaction mixture containing 20 mM HEPES (pH 7.6), 60 mM KCl, 1 mM $MgCl_2$ and 10% glycerol and chilled on ice. Then, $1\times10^5\sim10^6$ cpm of ^{32}P labeled RNA probe was added to make a total volume of 20 μl for further incubation at 30°C for 10 min. RNA-protein interactions were then stabilized by ultra-violet irradiation on ice for 30 min in CL-1000 UV cross-linker (UVP, Upland, CA, USA) set to an energy level of 1800 μJ/cm^2

with a distance of 8 cm[44], after which unbound RNA fragments were broken down by 1 μg/μl RNase A (QIAGEN GmbH, Hilden, Germany) and T1 (Roche diagnostic, Indianapolis, USA) at 37°C for 15 min. Each reaction was then mixed with 2 × SDS sample dissolving buffer (100 mM Tris-Cl, pH 6.8, 4% SDS, 0.2% bromphenol blue, 20% glycerol, 200 mM β-mercaptoethanol), boiled for 5 min and analyzed by 10% SDS-polyacrylamide electrophoretic gel. The gels were dried under vacuum at 50°C for 2 hours and imaged by autoradiography in a dark room using Fuji medical X-ray film "super RX" (Fuji photo film, Tokyo, Japan), X-ray developer and X-ray fixer (Vivid, Seoul, Korea).

2.11. Purification and identification eNOS mRNA-binding proteins

RNA-protein bindings were performed essentially as described by Mamatha Garige[45] with slight modifications. Ten μg of biotinylated RNA probe was incubated with 50 μl (500μg) of cell extract for 30 min at room temperature in a binding buffer (10 mM HEPES, pH 7.5, 25 mM KCl, 10% glycerol, and 1 mM dithiothreitol), after which unbound RNA fragments were broken down by 1 μg/μl RNase A (QIAGEN GmbH, Hilden, Germany) and T1 (Roche diagnostic, Indianapolis, USA) at 37°C for 15 min. Streptavidin magnetic beads (New England Biolabs, Beverly, MA, USA) were resuspended by gently flicking and inverting the bottle until the particles are completely dispersed. Then 30 μl of beads were washed in the binding buffer (lacking glycerol). Resuspended beads were added to the binding reaction for 25 min at room temperature with gently mixing by inversion every 1-3 min. The magnetic beads with immobilized RNA and its bound proteins were separated from crude cell extract on a magnetic stand. The RNA-protein complex bound to the magnetic beads was washed twice with the binding buffer. Then proteins were eluted by boiling for 5 min in 50 μl sample buffer (62.5 mM Tris-HCl, pH 6.8, 25% glycerol, 2% SDS, 0.01% bromphenol blue and 1% 2-mercaptoethanol). After applying magnetic field, the supernatant was loaded onto a 10% SDS-PAGE. The gel was stained with Coomassie Brilliant Blue for 2 hours and destained in a destaining solution of 50% methanol, 10% glacial acetic acid for 4 hours.

After confirming the RNA-bound protein band, the same experiment was done by two-dimensional gel electrophoresis (NEPHGE). As described above, RNA-protein-beads complex was washed twice in the binding buffer, then proteins were eluted by boiling for 5 min in 50 µl sample buffer without bromphenol blue (62.5 mM Tris-HCl, pH 6.8, 25% glycerol, 2% SDS, and 1% 2-mercaptoethanol). The supernatant was transferred to a new Eppendorf tube, after which BSA was added to a final concentration of 200 µg/ml. Two volumes of ice-cold ethanol containing 10 mM $MgCl_2$ were added to precipitate proteins at -70°C for at least 2 hours. After centrifugation (12,000 rpm) at 4°C for 10 min, protein pellets were dissolved in 20 µl isoelectric focusing (IEF) sample buffer containing 9 M urea (Promega, Madison, WI, USA), 5% ampholine (pH 3.5-10.0, Sigma Chemical Co, St. Louis, MO, USA), 0.02 M DTT and 2% Nonidet P-40 and then infused onto the IEF gel which was the first-dimensional separation of two-dimensional gel electrophoresis. IEF running gel was prepared in a long (15-cm), thin (1.2-mm) capillary tube by infusing the running gel solution into it. For one tube gel, a total volume of 1.25 ml of running gel solution was prepared, which was composed of 0.68 g urea, 0.05 ml distilled water, 167 µl O`Farrell solution (28.38% acrylamide, 1.62% bisacrylamide), 62.5 µl Ampholine (pH 3.5-10.0), 2.5 µl Ammonium Persulfate (Sigma Chemical Co, St. Louis, MO, USA) and 1.25 µl TEMED (Sigma Chemical Co, St. Louis, MO, USA). A 1.5-cm blank was left from the top of the capillary tube when introducing the appropriate volume of running gel solution into it and then air bubbles were removed by gently tapping the bottom of the tube. After which, distilled water (5~10 µl) was infused onto the gel solution using a Hamilton microsyringe (Hamilton Company, Reno, Nevada, USA). After gel formation, distilled water was removed. Then the IEF tube was assembled into the IEF apparatus and 10 µl of overlay buffer (7 M urea) was added following infusing protein samples to the IEF tube using the Hamilton microsyringe. Afterwards, the appropriate chambers were filled with upper (0.01 M H_3PO_4, anode) and lower (0.02 N NaOH, cathode) electrode buffers, respectively. IEF gel was run at the voltage condition of 50 V for 15 min, 100 V for 15 min, 200 V for 15 min, and 800 V for 3 hr. After IEF, the gel was removed from the capillary tube by injecting water around gels, then the gel was briefly equilibrated in a equilibration buffer (0.075M Tris, pH 6.8, 2.3% SDS, and 1% 2-mercaptoethanol) for 10~20 min and placed directly onto the top edge of a second-dimensional slab gel. In

addition, the control IEF gel, into which distilled water was introduced instead of protein samples, was cutted into pieces (approximate 0.5-cm / per piece) after electrophoresis and immersed into distilled water for at least 30 min to measure the pH of every pieces respectively using a pH Meter Model 420 A (Orion Research Inc., Boston, USA). By measuring the pH gradient across the gel and recording the approximate positions of every pieces, we can estimate the approximate pI of our target protein spot, information which could be valuable in determining the identity of the protein. The second-dimensional 10% polyacrylamide gel was stained with Coomassie Brilliant Blue as described above. Then the target protein spot was excised from the gel and MALDI-TOF spectrum was performed to identify the protein.

2.12. Statistics

All results were presented as means ± SEM. Statistical analysis were performed by unpaired student's t-test with GraphPad Prism programme ver.4.0 (GraphPad software Inc., San Diego, CA, USA). *P* values less than 0.05 were considered to be significant.

Ⅲ. Results

3.1. Identification of the more detailed locations of cis-elements in some regions of human eNOS mRNA.

Previously, we have reported that lovastatin increased the levels of eNOS mRNAs by exhausting intracellular GGPP. The cis-acting elements mediating such effects were located in heNOS-D sequence [2979-4341, based on the sequence of heNOS cDNA (gene bank #NM_000603)] (Figure 6).

To determine the more detailed locations of cis-elements compared to the previous experiments, we inserted three shorter eNOS-D fragments (heNOS_D1, D2, D3) into a mammalian expression vector pEGFP-C2/stop1.2 as described in Materials&Methods. The GFP vectors, alone or with heNOS_D1, D2, D3, were transiently transfected into EA.hy926 cells. The relative GFP mRNA levels were measured in the presence of lovastatin and isoprenoids by real-time PCR. As shown in figure 7, the relative mRNA levels of all three gene constructs heNOS_D1, D2, D3 were increased by lovastatin treatment. Either mevalonate or GGPP could prevent such effects of lovastatin. There was no change of control vector's GFP mRNA level in the presence of lovastatin and isoprenoids. The effects of lovastatin and isoprenoids on heNOS mRNA levels in every transfection experiments were also measured as a positive control. These data indicated that cis-elements mediating GGPP-induced decay of eNOS mRNA were dispersed at all three regions of D1, D2 and D3.

In order to identify the more detailed locations of cis-elements, a further subdivision of heNOS_D1 and D3 were performed. We constructed GFP constructs with six subdivided fragments (heNOS_D11, D12, D13, D31, D32, D33) to test them in transiently transfected EA.hy926 cells(Figure8 and 9). GFP relative mRNA level measurements by real-time PCR indicated that cis-acting elements mediating

GGPP-induced decay of eNOS mRNA were contained in both 3`UTR region (heNOS_D31, D32, D33) and the adjacent coding region (heNOS_D13). heNOS_D11 and D12 regions did not contain cis-elements.

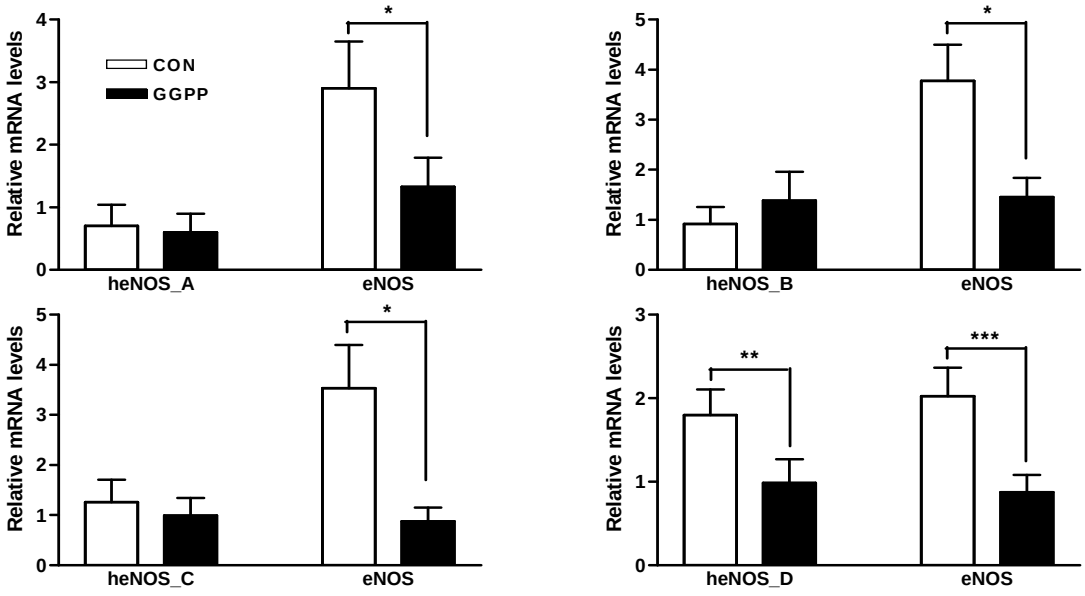

Fig. 6. The effects of lovastatin and GGPP on chimeric mRNA levels

EA.hy926 cells transfected with the chimeric gene construct containing a part of eNOS cDNA were cultured in a medium containing 10% DFBS and 25 μM lovastatin for 48 hours. GGPP was added to the medium at a concentration of 20 μM. As a control (CON), cells were cultured without GGPP. Results are expressed as means ± S.E.M. of two independent experiments, performed in triplicate. The data shown are ratios of the treated versus those of the corresponding FBS-control levels. *$P < 0.05$, ** $P < 0.01$, *** $P < 0.001$.

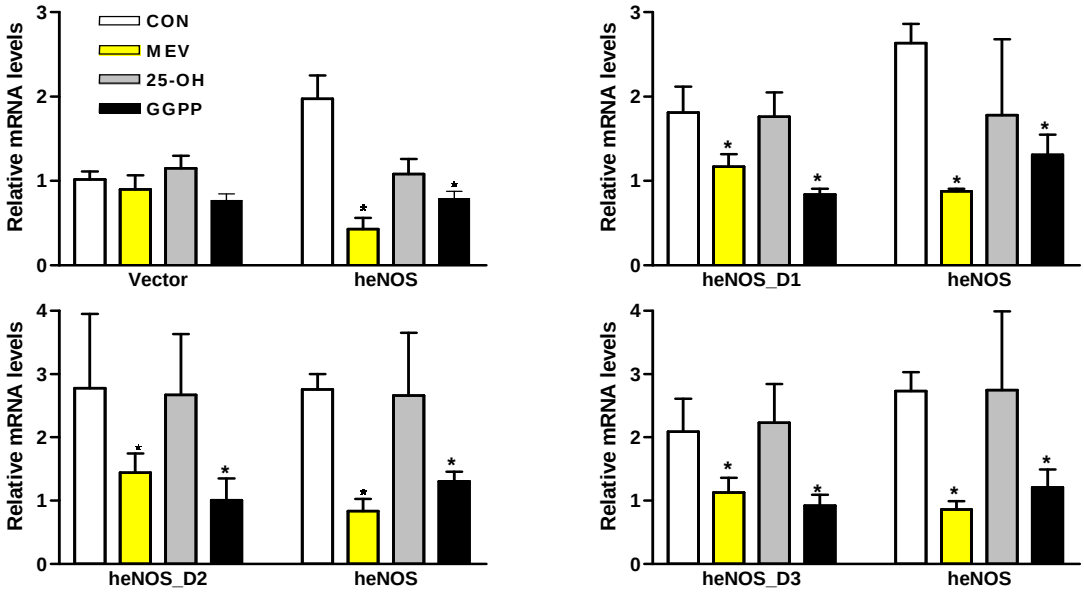

Fig. 7. The effects of lovastatin and sterols on the levels of chimeric mRNA containing a part of heNOS_D

EA.hy926 cells transfected with the chimeric gene construct containing a part of eNOS_D cDNA were cultured in a medium containing 10% DFBS and 25 μM lovastatin for 48 hours. When necessary, 25-hydroxycholesterol, mevalonate or GGPP was added to the medium at a concentration of 1.2 μM, 300 μM, or 20 μM respectively. As a control (CON), cells were cultured without sterols. The results are means ± S.E.M. of three independent experiments, each performed in duplicate. The data shown are ratios of the treated versus those of the corresponding FBS-control levels. * $P < 0.05$ as compared with each control.

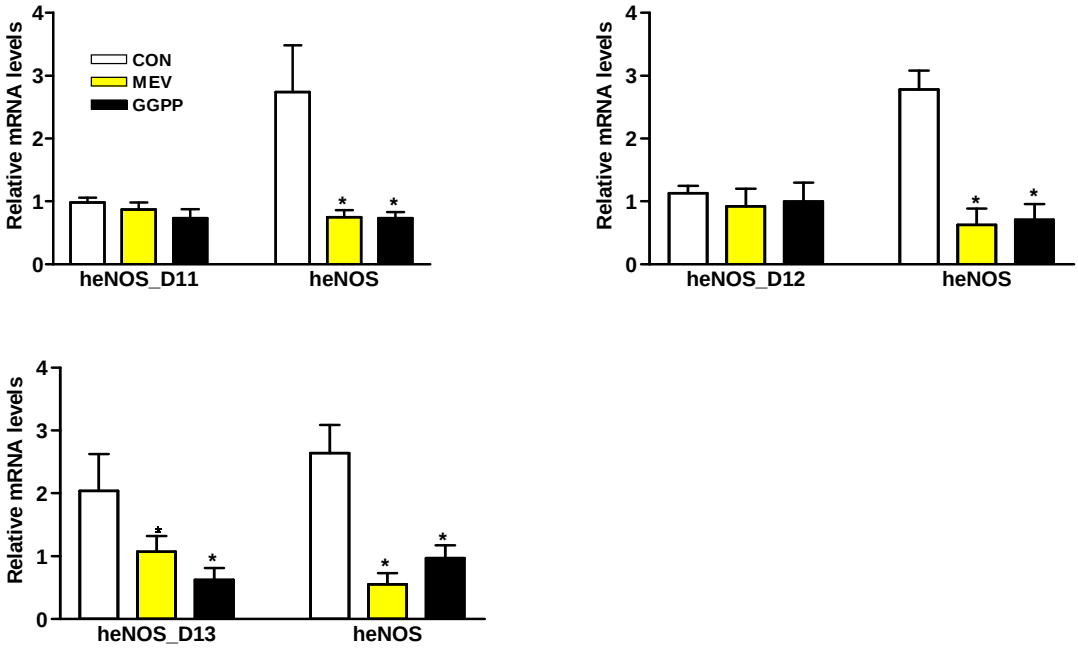

Fig. 8. The effects of lovastatin and sterols on the levels of chimeric mRNA containing a part of heNOS_D1

Cells transfected with the chimeric gene construct containing a part of eNOS_D1 cDNA were cultured in a medium containing 10% DFBS and 25 μM lovastatin for 48 hours. When necessary, mevalonate or GGPP was added to the medium at a concentration of 300 μM or 20 μM respectively. As a control (CON), cells were cultured without sterols. The results are means ± S.E.M. of three independent experiments, each performed in duplicate. The data shown are ratios of the treated versus those of FBS-control levels. * $P < 0.05$ as compared with each control.

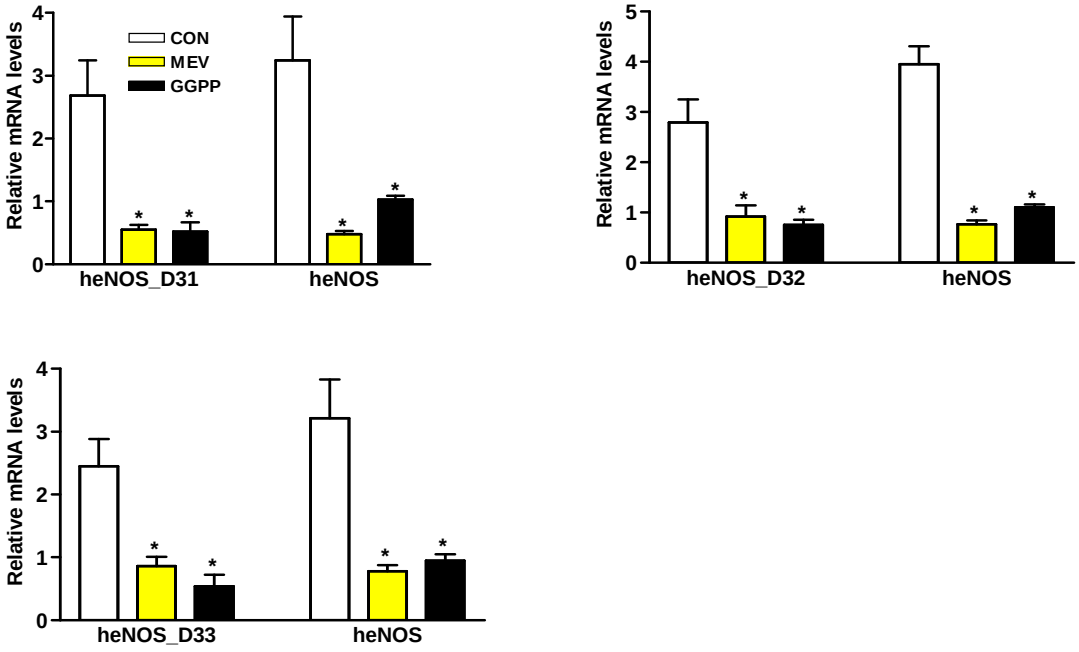

Fig. 9. The effects of lovastatin and sterols on the levels of chimeric mRNA containing a part of heNOS_D3

Cells transfected with the chimeric gene construct containing a part of eNOS_D3 cDNA were cultured in a medium containing 10% DFBS and 25 μM lovastatin for 48 hours. When necessary, mevalonate or GGPP was added to the medium at a concentration of 300 μM or 20 μM respectively. As a control (CON), cells were cultured without sterols. The results are means ± S.E.M. of three independent experiments, each performed in duplicate. The data shown are ratios of the treated versus those of FBS-control levels. * $P < 0.05$ as compared with each control.

3.2. Investigation of the more detailed regulatory mechanism of statin-mediated eNOS mRNA stability

It is known that geranylgeranylation is required for the activation and membrane targeting of small GTPases, including RhoA. The active membrane-bound form of RhoA elicits downstream signaling, which influences cytoskeleton organization. It has been reported that eNOS expression is regulated by changes in the actin cytoskeleton[46]. In order to determine whether effects of lovastatin on eNOS mRNA regulation are mediated by intracellular signaling pathways, the relative GFP mRNA levels of seven chimeric gene construct (heNOS_D11, D12, D13, D2, D31, D32, D33) were measured in the presence of either hydroxyfasudil, the Rho inhibitor, or cytochalasin D, a cytoskeleton disruptor by real-time PCR. As shown in figure 10, the relative GFP mRNA levels of D13, D2, D31, D32, and D33 gene constructs were increased in the presence of hydroxyfasudil or cytochalasin D. These data were in accordance with that of lovastatin treatment and indicated that cis-acting elements regulating eNOS mRNA stability were contained in both 3`UTR region (heNOS_D31,D32,D33) and the adjacent coding region (heNOS_D2,D13). Also, the status of cellular architecture regulated by Rho-mediated pathways may plays a role in determining the decay rate of eNOS mRNA.

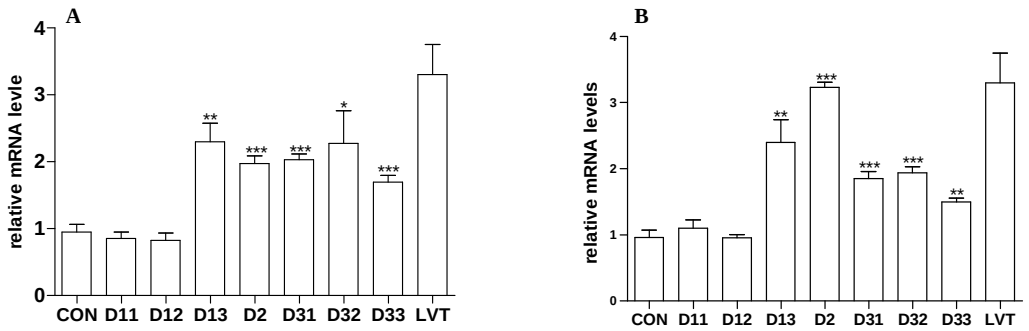

Fig. 10. The effects of hydroxyfasudil and cytochalasin D on the levels of chimeric mRNA containing a part of heNOS_D

Cells transfected with the chimeric gene construct were cultured in a medium containing 10% FBS for 48 hours. Hydroxyfasudil (A) or cytochalasin D (B) was added to the medium at a concentration of 10 μM or 1 μM respectively. CON shows the levels of GFP/vector mRNA, D11 shows the levels of GFP/heNOS_D11 mRNA and so forth. LVT shows the levels of eNOS mRNA when cells were cultured in a medium containing 10% DFBS and 25 μM lovastatin for 48 hours. The results are means ± S.E.M. of three independent experiments, each performed in duplicate. The data shown are ratios of the treated versus those of the corresponding FBS-control levels. *$P < 0.05$, ** $P < 0.01$, *** $P < 0.001$.

3.3. RNA-protein binding interactions by using RNA fragments encoding a part of heNOS_D cDNA

To confirm whether cis-acting elements at both coding and 3`UTR regions of eNOS mRNA bind with trans-acting factors, Cross-linking experiments were performed with in vitro transcribed and radiolabelled RNA fragments encoding D11, D12, D13, D21, D2, D31, D32, and D33 sequence (Figure 11). When radiolabelled RNA fragments were incubated with EA.hy926 cell lysates, multiple bands were observed. In cell lysates treated 48 hrs with lovastatin, the bindings of one RNP complex corresponding to approximate molecular weight of 60 kDa to D13, D2, D31, D32, D33 fragments were increased than in extracts from untreated control cells, therefore, this binding was considered as specific. However, D11, D12, and D21 fragments displayed very weak binding to this 60 kDa RNP, and there were no changes of binding activity after lovastatin treatment, accordingly this weak binding was considered as non-specific and might attributable to the high sensitivity of radioisotope. The binding of other bands were also not consistently changed after lovastatin treatment, thereby considered as non-specific binding which may attributable to high abundance of some proteins in cell lysates and not subjected to further investigation. No distinct bands could be observed from control reactions performed without cell lysates, demonstrating that the bands were not attributable to incompletely digested RNA fragments (Figure 11D). These data were in accordance with transfection data, further indicating that cis-acting elements regulating eNOS mRNA stability were contained in D13, D31, D32, D33, and the distal region of D2. In addition, binding of a 60 kDa RNP to cis-elements may play a role in the regulation of eNOS mRNA stability by lovastatin. Interestingly, D13, D2, D31, D32, D33 fragments all bind with one same 60 kDa trans-acting protein, consequently, we hypothesized D13, D2, D31, D32, D33 must contain the similar cis-acting elements or the similar secondary RNA structure which can bind with one same protein that contributes to the effect of lovastatin on eNOS. And this trans-acting protein is a

stabilizing factor.

In order to confirm the role of the status of cellular architecture in determining eNOS mRNA stability, the effects of cytochalasin D on the binding activities of cell lysates to the riboprobes were examined. As shown in Figure 12, in cell lysates treated 48 hrs with cytochalasin D, the bindings of the 60 kDa RNP to D13, D2, D31, D32, D33 fragments were increased than in extracts from untreated control cells. This data was also in accordance with that of lovastatin treatment, further confirming all the five fragments contain cis-elements and suggesting the status of cellular architecture has a role in determining eNOS mRNA stability.

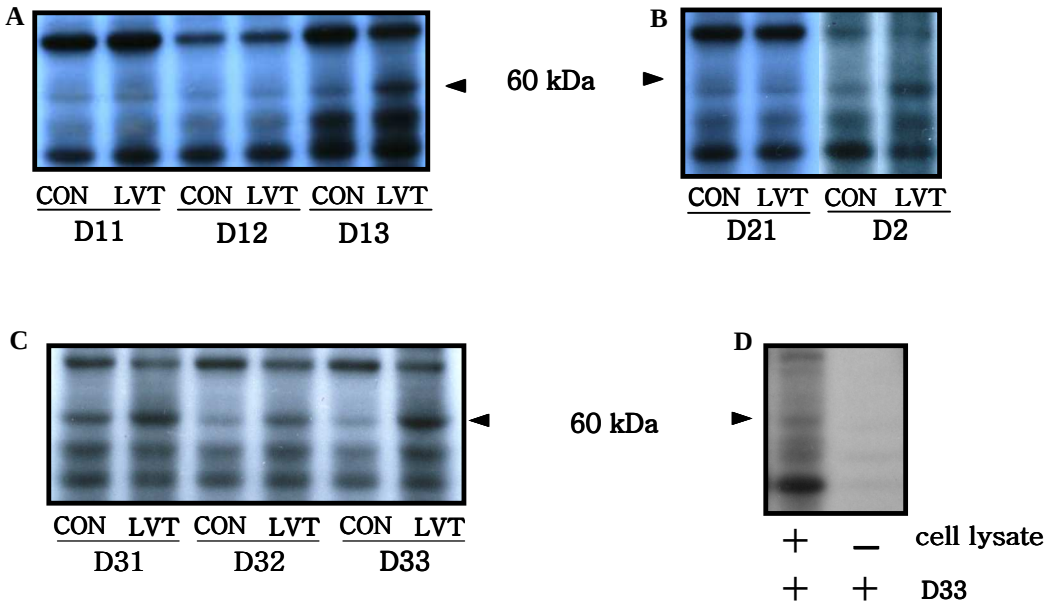

Fig. 11. The effects of lovastatin on RNA-protein interactions by using RNA fragments encoding a part of heNOS_D cDNA

RNA-protein cross-linking experiments using radiolabelled RNA encoding a part of eNOS cDNA. CON, control; LVT, 25 μM lovastatin treatment for 48 hours. D13 CON shows cross-linking studies using radiolabelled D13 RNA fragment with untreated cell lysate and so forth. (D) A representative experiment using radiolabelled D33 fragment in the absence or presence of cell extracts.

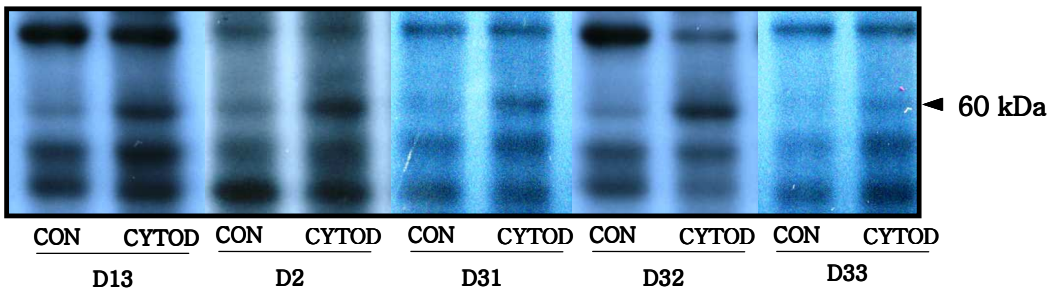

Fig. 12. The effects of cytochalasin D on RNA-protein interactions by using RNA fragments encoding a part of heNOS_D cDNA

RNA-protein cross-linking experiments using radiolabelled RNA encoding a part of eNOS cDNA. CON, control; CYTOD, 1 μM cytochalasin D treatment for 48 hours. D13 CON shows cross-linking studies using radiolabelled D13 RNA fragment with untreated cell lysate and so forth.

3.4. Determination of the exact locations of cis-elements in eNOS mRNA sequence

Unfortunately, we did not find the similar stem-loop secondary RNA structure after analyzing the secondary RNA structure of D13, D2, D31, D32, and D33 by using a RNA structure programme ver.4.4 (David H. Mathews, Isis Pharmaceuticals, Inc., Carlsbad, CA, USA). Thereby we speculated the binding of trans-acting factor to RNA fragments might be sequence specific. In order to identify the essential sequences of cis-acting elements, we avoided shortening of those fragments and carried out site-directed mutagenesis on every fragments. This was achieved by PCR-mediated mutagenesis replacing 4 or 5 nucleotides by a reported non-functional sequence as described in Materials&Methods.

CCUCU,UUCUC,CUUU motifs were reported to be the binding sequence for a 56kDa RNP complex on the 3`UTR of human eNOS mRNA, and the binding of the 56kDa factor to heNOS mRNA was required in the TNF-α induced mRNA downregulation. The 56kDa factor was speculated to be related to polypyrimidine tract binding(PTB) protein[28]. Also, one conserved copy of the CCUCC motif was previously reported to be the binding sequence for a 39-kDa RNP complex on the human α–globin mRNA, and the RNP complex had functional importance in establishing high-level stability of α-globin mRNA[39]. We found multiple CU-rich regions which contain reported CU-rich elements in the heNOS-D cDNA sequence as described in Materials&Methods. To show the functionality of the CU-rich elements, the resulting 19 mutants, D13 mutant 1 to 3, D2 mutant 1 to 3, D31 mutant 1 to 5, D32 mutant 1 to 5 and D33 mutant 1 to 3 were made as described in Materials&Methods, and then the function was tested in transiently transfected EA.hy926 cells by measuring their relative mRNA level using real-time PCR.

As shown in Table 13, D13 wild-type contains two adjacent CU-rich elements. When one of the elements or both of them were mutated (D13 mutant 1, 2 and 3), GFP relative mRNA levels showed no varieties in the presence of lovastatin while wild-type gave a significant increase of relative mRNA level(Figure 13A). This suggested that both two elements were important for maintaining the stabilizing function of D13

fragment. The function would be completely lost once one element was mutated, this means, only one element was not enough to maintain the function. Consequently, cooperation of two adjacent CU-rich elements UCCUC and UUCUC was necessary for maintaining their stabilizing function.

D2 wild-type and its mutants exhibited similar variational patterns of relative mRNA levels with D13 (Figure 13B), which indicated that two adjacent elements CUUU and UCCUU need to cooperate to maintain their stabilizing function. D33 wild-type and its mutants also exhibited similar variational patterns of relative mRNA levels with D13 (Figure 13E), which also suggested that cooperation of two adjacent CU-rich elements CCUCU and CCUCU was necessary for maintaining their stabilizing function.

D31 wild-type contains three CU-rich elements, CUUU (named element 1), CCUCC (named element 2) and CCUCU (named element 3). Elements 2 and 3 are adjacent (shown in Materials&Methods). As shown in Figure 13C, D31 mutant 5 (mutating all of the three elements) did not give any function, however, when element 1, CUUU, was mutated (D31 mutant1), the function was still remained. This suggested that elements 2 and 3 showed function in D31 fragment. While element 2, CCUCC, was mutated (D31 mutant 2), the function was lost, whereas, the mutation of element 3 (D31 mutant 3) did not affect the function. This suggested that element 2, CCUCC, was very important for maintaining function. As expectly, mutation of both elements 2 and 3 (D31 mutant 4) lead to the loss of the stabilizing function, attributing to the loss of element 2, CCUCC.

D32 wild-type contains three CU-rich elements, CCUCU, CCUCU, and CCUCC. The first two elements are adjacent. As shown in Figure 13D, D32 mutant 5 (mutating all of the three elements) did not give any function, while mutant 4 (mutating the first two elements) was functional, implicating that the existence of the third element, CCUCC, play a role in maintaining the stabilizing function. Mutant 3 (mutating the third element) was functional, suggesting that CCUCU, CCUCU could also maintain

the function. Mutant 1 and 2 were both functional, attributing to the existence of the third functional element CCUCC. However, whether the function of CCUCU and CCUCU was cooperative or separative is still uncertain. According to the data of D33 mutants, the function of CCUCU and CCUCU was considered as cooperation. These data revealed that two adjacent CU-rich elements CCUCU and CCUCU were able to maintain their stabilizing function, and the existence of CCUCC also played a role in stabilizing eNOS mRNA.

In order to confirm whether Rho pathway play a role in the regulation of CU-rich elements mediated stability of eNOS mRNA, the effects of hydroxyfasudil on the levels of chimeric mRNAs containing part of heNOS_D or their mutants were tested in transiently transfected EA.hy926 cells by measuring their relative mRNA level using real-time PCR. We can see from Figure 14, the effects of hydroxyfasudil were totally in accordance with the effects of lovastatin on the chimeric mRNA levels. We concluded that Rho-mediated pathway affects eNOS mRNA stability, which is mediated by multiple CU-rich elements located in the 3´UTR and adjacent coding regions of eNOS mRNA.

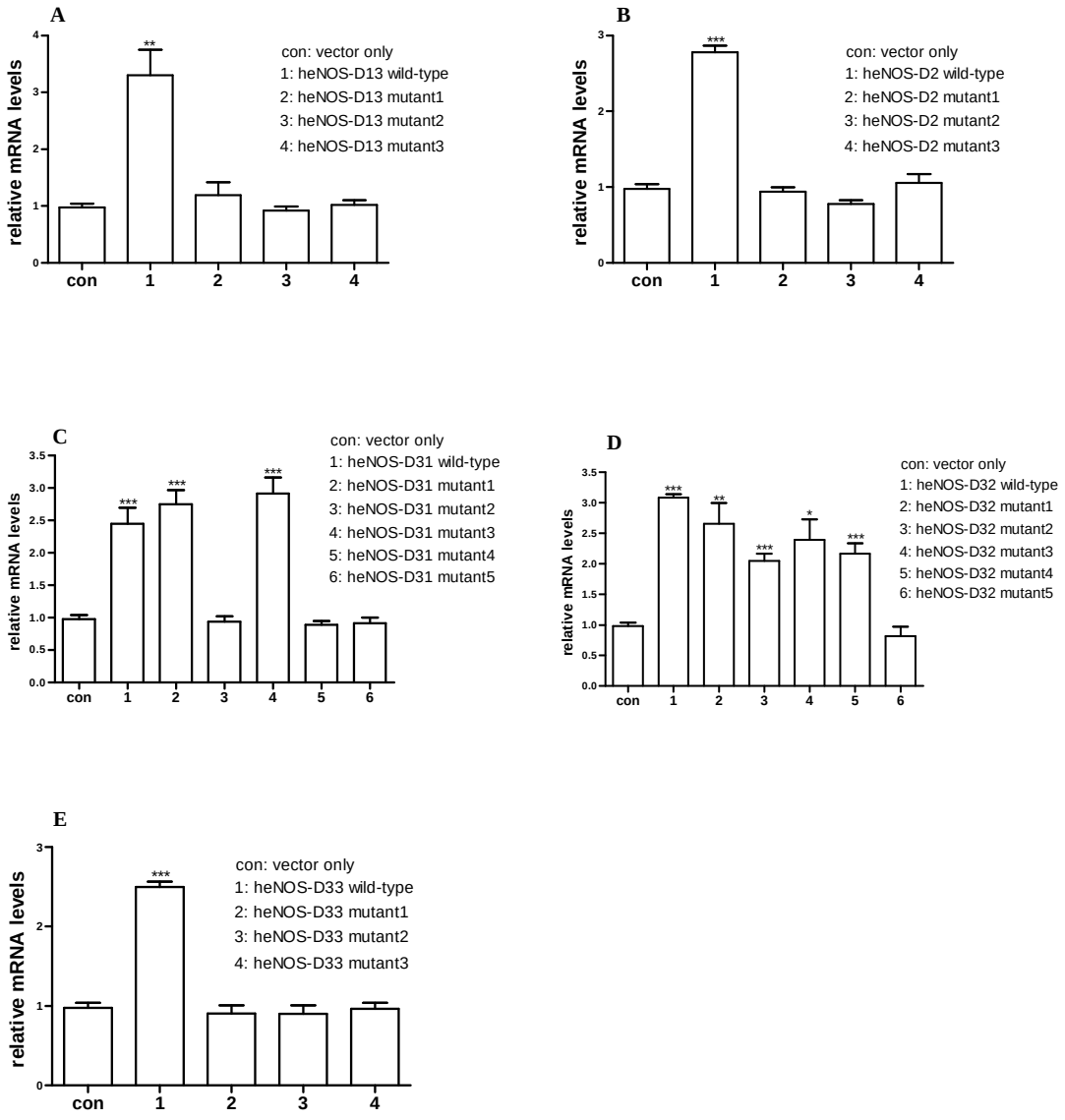

Fig. 13. The effects of lovastatin on the levels of chimeric mRNA containing a part of heNOS_D or their mutants

Cells transfected with the chimeric gene construct containing a part of eNOS_D cDNA fragments or their mutants were cultured in a medium containing 10% DFBS and 25 μM lovastatin for 48 hours. Mutants were made by substituting CU-rich elements as described in Materials&Methods. The results are means ± S.E.M. of three independent experiments, each performed in duplicate. *$P < 0.05$, ** $P < 0.01$, *** $P < 0.001$.

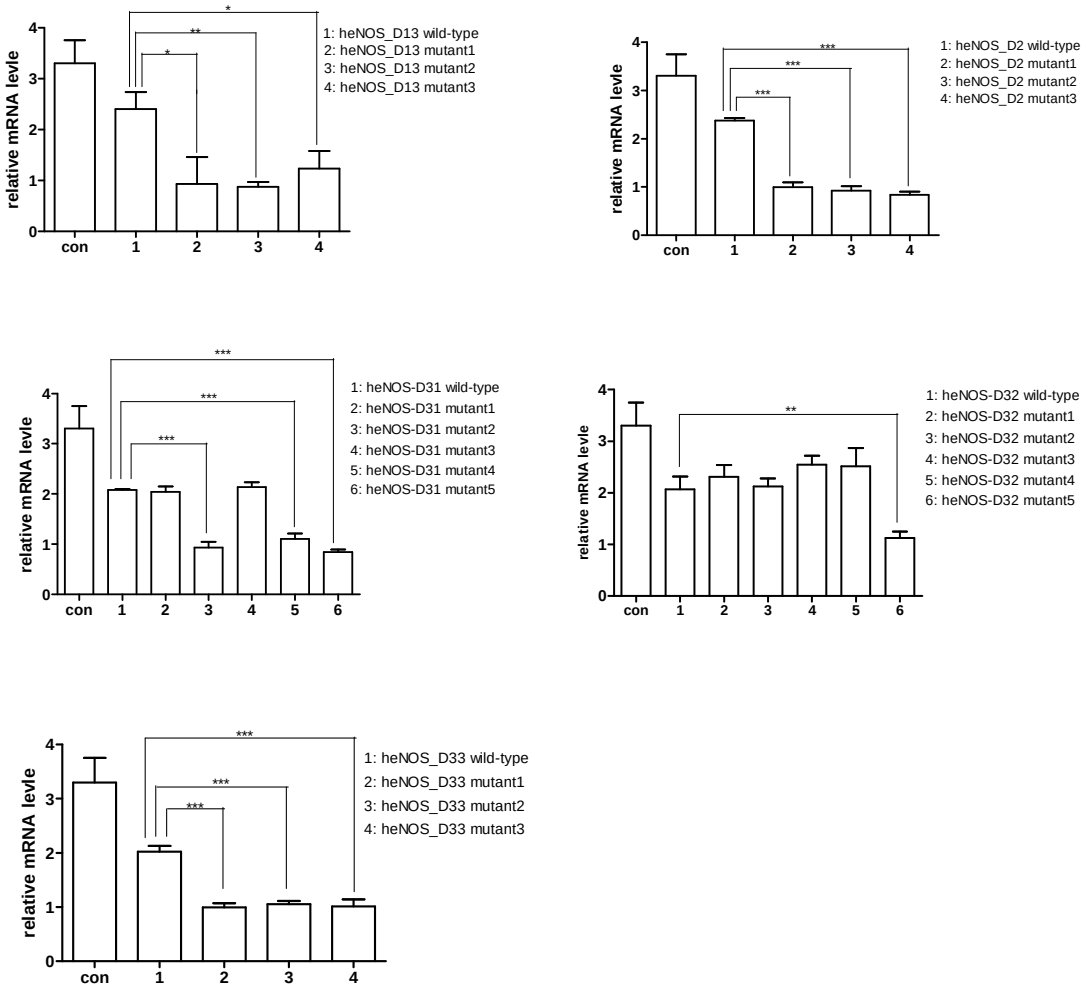

Fig. 14. The effects of hydroxyfasudil on the levels of chimeric mRNAs containing a part of heNOS_D or their mutants

Cells transfected with the chimeric gene construct containing a part of eNOS_D cDNA fragments or their mutants were cultured in a medium containing 10% FBS for 48 hours. Hydroxyfasudil was added to the medium at a concentration of 10 μM. CON shows the levels of eNOS mRNA when cells were cultured in a medium containing 10% DFBS and 25 μM lovastatin for 48 hours. Mutants were made as described in Materials&Methods. The results are means ± S.E.M. of three independent experiments, each performed in duplicate. *$P < 0.05$, ** $P < 0.01$, *** $P < 0.001$.

3.5. RNA-protein binding interactions by using mutated RNA fragments

To confirm whether trans-acting factors bind with CU-rich elements, cross-linking experiments were performed with in vitro transcribed and radiolabelled RNA fragments encoding D13, D2, D31, D32, D33 sequences and their mutants (Figure 15).

D13, D2 and D33 mutants displayed weak bindings to that 60 kDa RNP, and there were no changes of binding activities after lovastatin treatment (Figure 15A, B, E), therefore, these weak bindings were considered as non-specific and might attributable to the high sensitivity of radioisotope . This suggested that, when the cooperative CU-rich elements were mutated, the corresponding RNA probes lost their binding ability.

In cell lysates treated 48 hrs with lovastatin, the bindings of the 60 kDa RNP complex to D31 mutant 1 and 3 were increased than in extracts from untreated control cells (Figure 15C). However, D31 mutant 2, 4 and 5 exhibited very weak binding to that 60 kDa RNP, which was not in response to lovastatin treatment and considered as non-specific binding. This suggested that the existence of CCUCC element was crucial for binding of trans-acting factor to D31 fragment.

D32 mutant 1, 2, 3 and 4 probes did not lose their binding ability, which could be increased by lovastatin treatment, while mutation of all three elements (mutant 5) do affected the binding (Figure 15D), strongly suggesting that cooperation of two adjacent elements, CCUCU and CCUCU, played a role in binding of trans-acting factor to D32 fragment. And, the existence of CCUCC element also had a role in binding of trans-acting factor to D32 fragment.

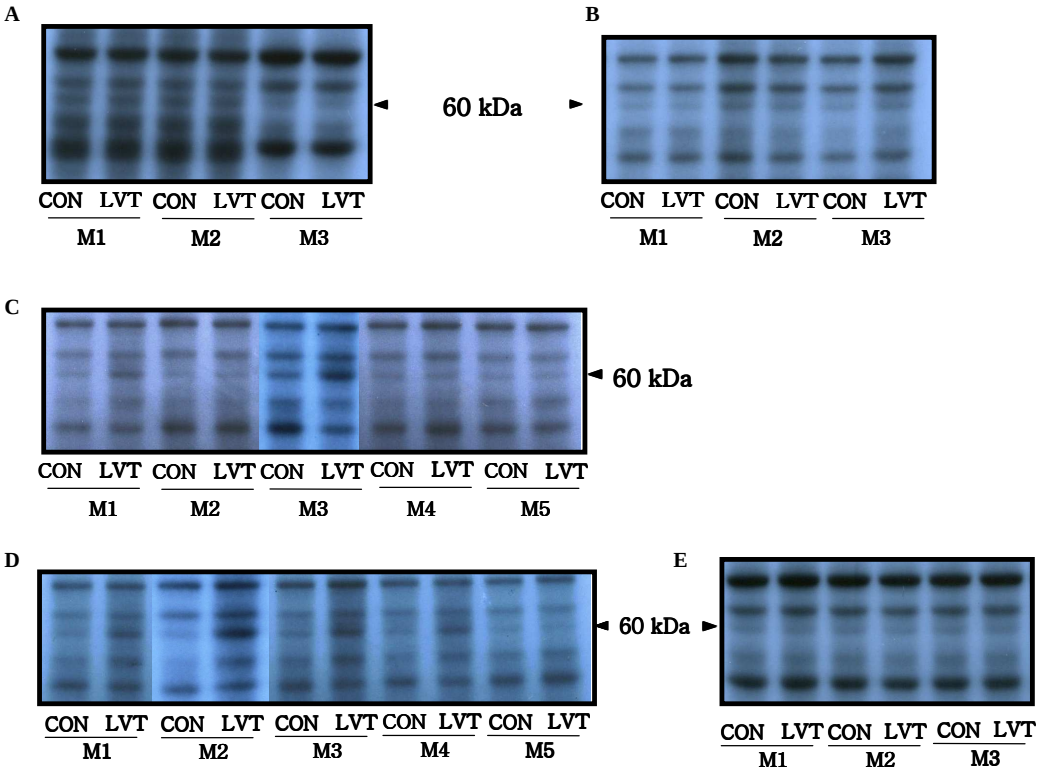

Fig. 15. The effects of lovastatin on RNA-protein interactions by using RNA fragments encoding D13, D2, D31, D32 and D33 mutants

RNA-protein cross-linking experiments using radiolabelled RNA encoding D13, D2, D31, D32 and D33 mutants. CON, control; LVT, 25 μM lovastatin treatment for 48 hours. (A, B, C, D, E) Cross-linking studies using radiolabelled D13, D2, D31, D32 and D33 mutants respectively. M 1 CON shows cross-linking studies using radiolabelled mutant 1 RNA fragment with untreated cell lysate and so forth.

3.6. Identification of the trans-acting factor which binds to the cis-elements of eNOS mRNA

In order to determine the identity of the 60 kDa RNP complex, Biotin-labelled D33 wild-type RNA probe was used along with D33 mutant 3 probe to study the specificity of their binding to EA.hy926 cell lysates. As shown in Figure 16, a band corresponding to 60kDa was found only with D33 wild-type probe (lane 4) but not with D33 mutant 3 probe (lane 3) under identical conditions. As expected, in cell lysates treated with lovastatin, the binding of the 60 kDa RNP complex to D33 wild-type was increased than in extracts from untreated control cells (lane 4 and 5). Lane 1 and 2 showed same amount of untreated and lovastatin treated cell lysates. And we can see there were no differences of the amount, demonstrating that the increase of the binding in the presence of lovastatin was specifically due to the effect of the drug and not due to differences between cell lysate amounts.

In order to separate and determine the identity of the 60 kDa RNP complex, two-dimensional gel electrophoresis were performed to analyze the protein profile after cross-linking experiments using biotin-labelled D33 wild-type and D33 mutant 3 RNA probes. As shown in Figure 17, three adjacent spots (indicated by black arrows) corresponding to approximate molecular weight of 60 kDa and pI value of 4.0-7.0 was found only with D33 wild-type probe (Figure C and D) but not with D33 mutant 3 probe (Figure B) under identical conditions. Also as expected, the binding of the 60 kDa RNP complex to D33 wild-type was increased in cell lysates treated with lovastatin than in extracts from untreated control cells (Figure C and D).

In order to purify and identify the eNOS mRNA binding protein, three adjacent spots corresponding to approximate 60 kDa were excised and MALDI-TOF spectrum technics were performed. Figure 18 shows the spectrum results of the central predominant spot. Analysis report (Figure B) indicated that β-actin was the predominant protein in that target spot. This suggested that β-actin was an integral part of the 60 kDa RNP that interacts with the eNOS mRNA fragment. Because of the intrinsic nature of

mass spectrometry, there may be other proteins in the sample that were not detected but were part of the RNP complex. Despite this possibility, the discrepancy in size between β-actin (41 kDa) and the 60 kDa protein may be attributable in part to the presence of a crosslinked fragment of eNOS mRNA. Unfortunately, we failed to determine the identity of the other two spots which locate at two sides. The failure is attributable to the weak density of them. Those two spots were considered to be the migration of the central predominant one.

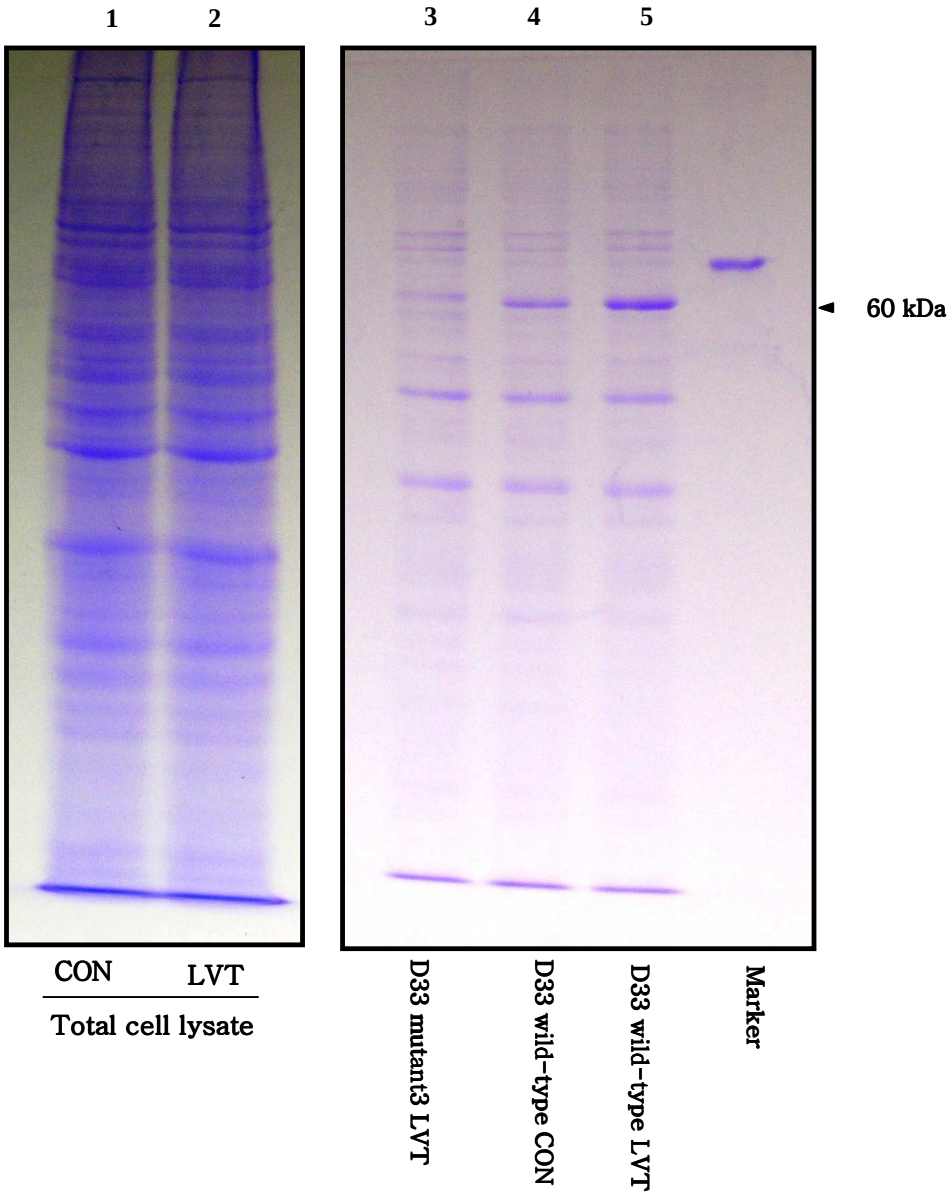

Fig. 16. Identification of RNA-binding protein by using biotin-labelled RNA probe

RNA-protein cross-linking experiments were performed by using biotin-labelled RNAs encoding D33 wild-type and D33 mutant 3. Riboprobe-bound proteins were separated by streptavidin magnetic beads. Protein profiles were analyzed by SDS-PAGE and Coomassie Brilliant Blue staining as described in Materials&Methods. CON, control; LVT, 25 μM lovastatin treatment for 48 hours. Lane 1 and 2 showed total cell lysate protein profiles of non-treated control and lovastatin treated groups. Lane 3, 4, 5 shows cross-linking studies using biotin-labelled RNA probes and treated or non-treated cell lysates.

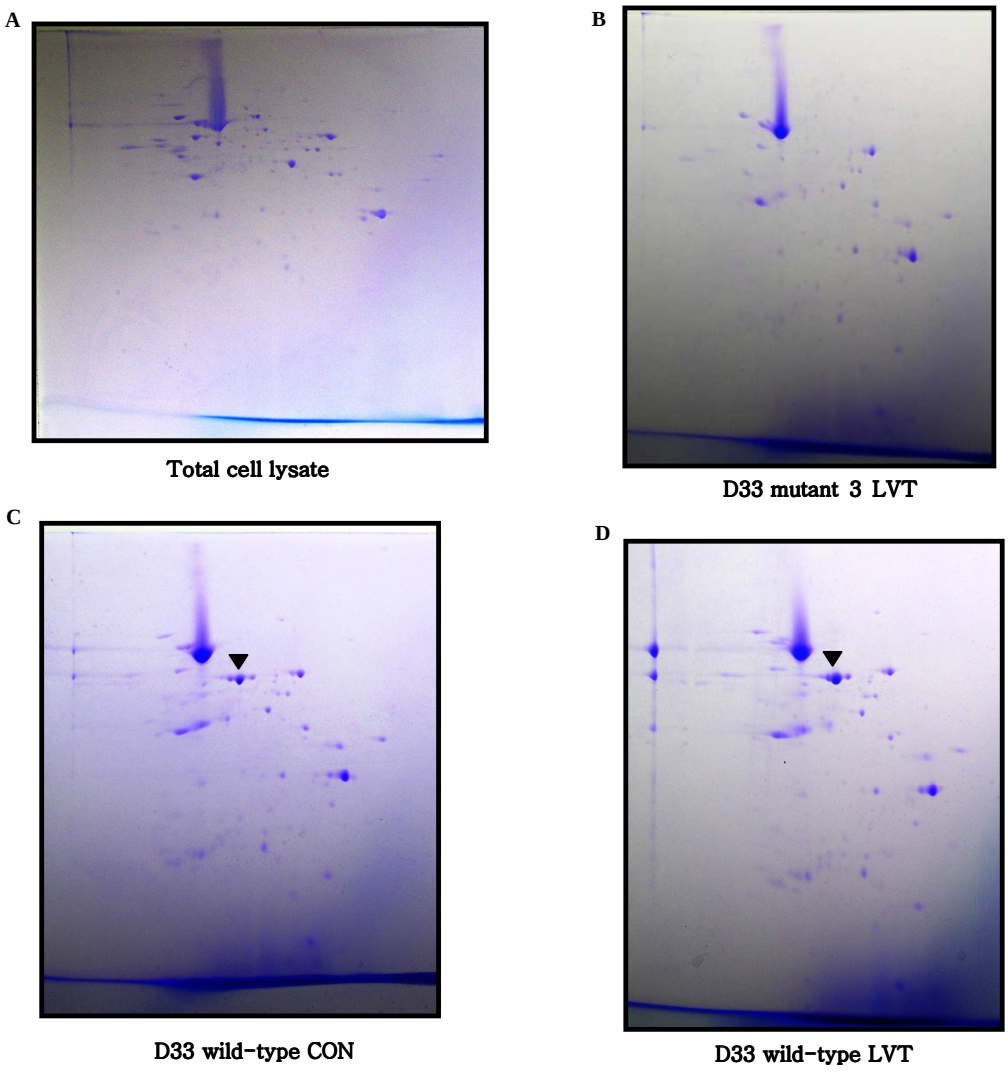

Fig. 17. Identification of RNA-binding protein by two-dimensional gel electrophoresis

RNA-protein cross-linking experiments were performed by using biotin-labelled RNAs encoding D33 wild-type and D33 mutant 3. Riboprobe-bound proteins were separated by streptavidin magnetic beads. Protein profiles were analyzed by two-dimensional gel electrophoresis and Coomassie Brilliant Blue staining as described in Materials&Methods. CON, control; LVT, 25 μM lovastatin treatment for 48 hours. (A) Protein profiles of non-treated control total cell lysate. (B, C, D) Cross-linking studies using biotin-labelled RNA probes and treated or non-treated cell lysates.

A

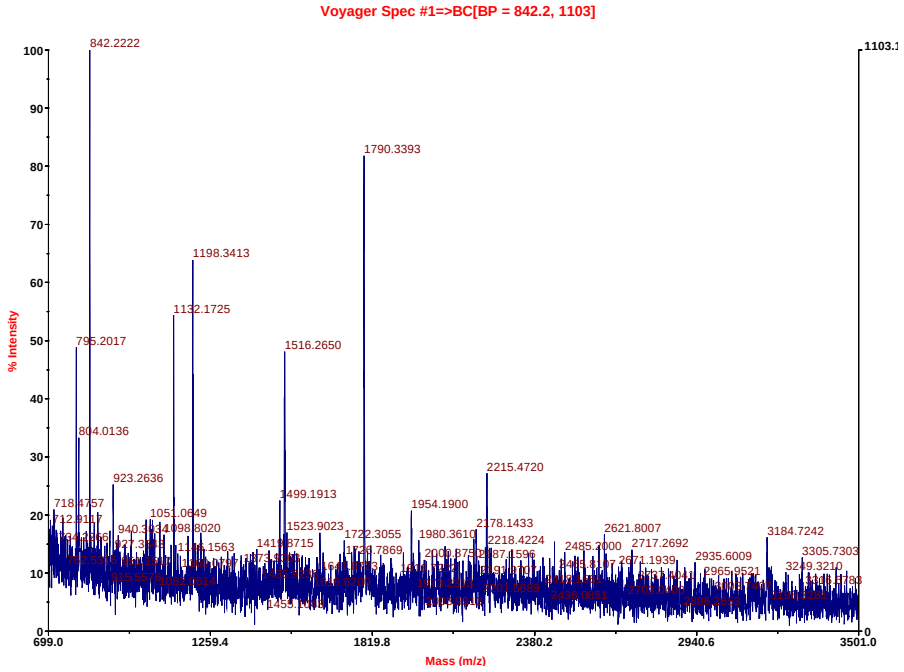

B

Concise Protein Summary Report

Format As | Concise Protein Summary | Help

Significance threshold p< 0.05 | Max. number of hits 20

Re-Search All | Search Unmatched

1. gi|15277503 **Mass:** 40194 **Score:** 93 **Expect:** 0.00011 **Queries matched:** 7
ACTB protein [Homo sapiens]
gi|14250401 **Mass:** 40978 **Score:** 92 **Expect:** 0.00012 **Queries matched:** 7
actin, beta [Homo sapiens]
gi|16924319 **Mass:** 40477 **Score:** 92 **Expect:** 0.00013 **Queries matched:** 7
Unknown (protein for IMAGE:3538275) [Homo sapiens]
gi|4501885 **Mass:** 41710 **Score:** 92 **Expect:** 0.00013 **Queries matched:** 7
beta actin [Homo sapiens]
gi|4501887 **Mass:** 41766 **Score:** 92 **Expect:** 0.00013 **Queries matched:** 7
actin, gamma 1 propeptide [Homo sapiens]
gi|62897671 **Mass:** 41694 **Score:** 92 **Expect:** 0.00013 **Queries matched:** 7
beta actin variant [Homo sapiens]
gi|62897409 **Mass:** 41696 **Score:** 92 **Expect:** 0.00013 **Queries matched:** 7
beta actin variant [Homo sapiens]
gi|62897625 **Mass:** 41738 **Score:** 91 **Expect:** 0.00016 **Queries matched:** 7
beta actin variant [Homo sapiens]
gi|16359158 **Mass:** 41736 **Score:** 71 **Expect:** 0.014 **Queries matched:** 6
Actin, beta [Homo sapiens]
gi|28336 **Mass:** 41786 **Score:** 70 **Expect:** 0.018 **Queries matched:** 6
mutant beta-actin (beta'-actin) [Homo sapiens]
gi|178045 **Mass:** 25862 **Score:** 63 **Expect:** 0.099 **Queries matched:** 5
gamma-actin

Fig. 18. Results of MALDI-TOF spectrum experiment

(A) Spectrum peptide peaks (B) Mascot Search Results: concise protein summary report by searching NCBI database.

Ⅳ Discussion

Posttranscriptional mechanisms play an important role in the regulation of expression of an increasing number of eukaryotic genes. Previously, we have reported the effects of lovastatin on the eNOS gene expression at the posttranscriptional level in EA.hy926 cells. Our data shows that lovastatin (25 μM) increased the levels of eNOS mRNA to approximately 3 fold. Among sterols examined in our experiments, either mevalonate (300 μM) or GGPP (20 μM) completely blocked the effects of lovastatin and significantly decreased eNOS mRNA half-life compared with the half-life of eNOS mRNA in lovastatin-treated cells. Our data indicates that either mevalonate or GGPP accelerated the decay of eNOS mRNA and lovastatin stabilized eNOS mRNA by depriving these intracellular sterols. We also proved that cis-acting elements, existed in the 3′ end of eNOS mRNA, are necessary for the regulation of eNOS mRNA decay.

In this experiment, we aimed to 1) characterize more detailed molecular mechanisms controlling eNOS mRNA stability, 2) determine precise sequences and exact locations of cis-acting elements, and 3) identify corresponding trans-acting factors that mediate sterol-responsive regulation of eNOS mRNA stability by using EA.hy926 cell line.

4.1. Characterizing more detailed molecular mechanisms controlling eNOS mRNA stability

It is known that GGPP serves as an important lipid attachments for the posttranslational modification and activation of a variety of signaling proteins. Included in this group of proteins are members of the Rho GTPase family[47]. The cytoskeleton is a downstream sensor of Rho GTPase, and each member of the Rho family serves specific functions in terms of cell shape, motility, secretion, and proliferation[48]. Therefore, effects of lovastatin on mRNA stability may be mediated by intracellular signaling pathways.

An association between actin cytoskeleton organization and eNOS expression has been described previously. HMG-CoA reductase inhibitors posttranslationally inhibit

Rho activity and upregulate eNOS expression posttranscriptionally[29]. Endothelial cells that overexpressed a dominant-negative Rho A mutant exhibited decreased actin stress fiber formation and increased eNOS expression[46]. Mice treated with a Rho inhibitor or the actin cytoskeleton disrupter cytochalasin D showed increased vascular eNOS expression and activity, and these changes were associated with a decrease in cerebral infarction size after middle cerebral artery occlusion[46]. In our experiment, either hydroxyfasudil (10 μmol/L), a Rho-kinase inhibitor, or cytochalasin D, a disrupter of the actin cytoskeleton, upregulated the levels of eNOS mRNA (Figure 10). These data indicates that the cellular architecture regulated by Rho-mediated pathways has a role in determining the decay rate of eNOS mRNA (shown in Figure 19). Laufs and Liao[49] found that Rho negatively regulates eNOS expression in human endothelial cells and treatment of endothelial cells with statins decreased the geranylgeranylation, membrane translocation, and GTP binding activity of Rho. Taking together, Alteration of Rho signaling by statins may lead to changes in endothelial actin cytoskeleton organization that affect the transport, localization, translation, and stability of eNOS mRNA. Furthermore, this mechanism that involves Rho signaling to stabilize eNOS mRNA is likely not unique to statins, Rho/Rho kinase inhibition has been shown to reverse the downregulation of eNOS that occurs in response to thrombin[50] and hypoxia[51].

4.2. Determining precise sequences and exact locations of cis-acting elements

In order to determine whether cis-acting elements are necessary for the regulation of eNOS mRNA stability, transfection experiments using chimeric gene constructs containing a part of eNOS cDNA were performed and the existence of cis-acting elements were confirmed. These cis-elements were dispersed at both 3′UTR and adjacent coding regions of eNOS mRNA. In order to determine precise sequences and exact locations of these cis-acting elements, several mutants corresponding to the hypothesized CU-rich elements were prepared. Our results showed that eNOS mRNA could be stabilized by lovastatin treatment in the presence of several CU-rich elements, while lovastatin failed to stabilize the mRNA mutants lacking CU-rich elements, strongly suggesting that CU-rich elements, UCCUC, UUCUC, CUUU, UCCUU,

CCUCC and CCUCU were functional in the regulation of eNOS mRNA stability in cultured human endothelial cells. In addition, these elements are not only responsible for the effect of lovastatin but also for hydroxyfasudil on eNOS mRNA stability. (Figure 13 and 14), further supporting that the effect of lovastatin on eNOS mRNA stability was mediated by Rho signal pathway (shown in Figure 19).

It has recently become apparent that mRNA decay is a highly regulated process involving interactions of cis-acting sequences and trans-acting factors. In this study, one 60 kDa RNP that specifically binds to eNOS 3'UTR RNA fragments have been identified in EA.hy926 cellular extracts. The binding of this protein increased significantly in response to lovastatin or cytochalasin D. However, at this point, it is not known if the changes in binding reflected changes in the binding affinity or the relative abundance of individual RNA-binding factors. Moreover, the mRNA binding of the 60 kDa RNP was found to be enhanced by lovastatin in a manner that correlates to the concomitant increases in eNOS mRNA abundance, suggesting but not establishing a causal relationship between the RNA-protein interaction and eNOS mRNA stability. Therefore, this trans-acting protein could represent suitable therapeutic targets to protect endothelial function.

The 60 kDa factor can be formed in the presence of cell lysates with CU-rich RNA fragments, as all RNA mutants lacking CU-rich elements failed to form it, suggesting that this 60 kDa binding factor has an affinity for RNA rich in CU-elements. The binding can be increased after treatment with lovastatin which upregulates eNOS mRNA expression by transcript stabilization, indicating that binding of 60 kDa RNP to CU-rich elements has functional importance in the regulation of eNOS mRNA stability. Together, these findings suggest that the interaction of the binding factor with CU-rich elements is associated with enhanced mRNA stability and the 60 kDa RNP is a stabilizing factor. There are also other reports which have shown that CU-rich motifs have a role in the regulation of eNOS mRNA stability[28]. However, whether this theory was also applicable to other genes is still uncertain. Future experiments of CU-rich elements/60 kDa RNP interaction may be needed to examine its role in mRNA stability of other genes, like 3-hydroxy-3-methyl-glutaryl-CoA reductase.

In bovine aortic endothelial cells, a CU-rich, 25 nt cis-element in the 5` half of the eNOS 3`UTR was identified to be the binding sequences for a 60 kDa cytoplasmic

protein[24, 27]. And also, a CU-rich region in bovine eNOS 3`UTR was shown to be the binding target for 51 and 60 kDa proteins from guinea pig pericardial extracts[52]. The functional roles of CU-rich binding regions have been observed in endothelial cells from different species and in response to different stimuli. In addition, the CU-rich region is highly conserved between human, bovine, and rabbit eNOS 3`UTRs[53]. Taken together, these observations suggest that the association between CU-rich region and RNP complex is part of a conserved pathway for eNOS mRNA stabilization. However, this work has shown only a relation between CU-rich region/RNP complex formation and mRNA stabilization, not causality. It remains to be proven that the 60 kDa protein directly participates in modulation of eNOS mRNA half-life.

4.3. Identifying corresponding trans-acting factors that mediate sterol-responsive regulation of eNOS mRNA stability

In order to determine the identity of this RNA-binding protein, UV-crosslinking studies using biotin-labelled RNA probes and two dimensional gel electrophoresis were performed. Analysis of Maldi-TOF spectrum identified β-actin protein as the major component of the ribonucleoprotein that binds to eNOS mRNA CU-rich elements.

We were unable to identify any other proteins in our ribonucleoprotein sample, but we cannot exclude that the interaction between actin and eNOS mRNA may be facilitated by actin-binding proteins. Further studies may be needed to investigate the molecular details of actin / eNOS mRNA association.

Our data showed that the binding of β-actin to CU-rich elements could be enhanced by cytochalasin D treatment or lovastatin treatment, further supporting that changes in the endothelial actin cytoskeleton organization may represent the mechanistic basis for the effect of lovastatin on eNOS mRNA stability.

In this study, we provide some insight that the status of cellular architecture of endothelial cells may regulate eNOS mRNA stability. β-actin may be a functional trans-acting factor for transcript stabilization. The molecular details of how the actin/eNOS mRNA interaction regulates eNOS mRNA stability and expression remains to be determined, but it may involve cytoskeletal-mediated mRNA transport,

localization, and subsequent translation. Future studies of the actin/eNOS mRNA interaction may be needed to examine its role in eNOS mRNA localization and metabolism.

It is known that RNA-binding proteins may serve dual roles. For example, GAPDH has been shown to bind to AU-rich regions of mRNAs and modulate RNA turnover in addition to its well-described role in glycolysis[54]. The iron-regulatory protein that recognizes transferrin and ferritin mRNAs is identical to aconitase, a Krebs cycle enzyme[55]. Likewise, heat shock protein-70 (HSP-70) has been shown to modulate turnover of erythropoietin mRNA in addition to its role in stress responses[56]. At present, the β-actin protein we have observed binding to the CU-rich elements is also a protein with other functions in forming the most dynamic one of the three subclasses of the cytoskeleton, which gives mechanical support to cells.

Many studies have shown that eNOS expression is influenced by several pathophysiological conditions via posttranscriptional mechanisms. These include exposure to hypoxia, oxidized LDL, and cytokines[10, 57-59]. The precise mechanisms involved in modulation of eNOS mRNA stability in these studies have not been determined. The present study indicates that eNOS mRNA expression is regulated via posttranscriptional mechanisms by lovastatin treatment, likely via interactions of actin and eNOS mRNA. Whether those various conditions share similar mechanisms of posttranscriptional regulation is unknown. One group has reported that interactions of actin and eNOS mRNA are involved in growth-related changes in eNOS mRNA stability[60]. Another group has characterized that either hydrogen peroxide or laminar shear stress modulates bovine eNOS mRNA stability and translation via increased 3` polyadenylation[61]. Interestingly, we find that lovastatin can not induce human eNOS 3` poly (A) tail lengthening (data not shown). Taken together, it suggests that some features of regulatory mechanisms for eNOS expression may be common to diverse stimuli, but there are also aspects of these mechanisms that are distinct for a given stimulus.

Demonstration of actin/eNOS mRNA association opens the door to the possibility that manipulation of the cytoskeleton may provide a new avenue for preventing or reversing impaired eNOS activity and vascular NO production. Regulation of eNOS expression by the actin cytoskeleton is a novel concept that may help to advance new

sights in the field of therapy for endothelial dysfunction.

In summary, we have identified one cellular factor β-actin with binding affinity for CU-rich RNA sequences in the human eNOS 3`UTR and adjacent coding regions as candidate regulatory trans-acting factors and cis-elements in the control of eNOS mRNA expression in cultured EA.hy926 cells. The binding of β-actin to regulatory CU-rich elements within eNOS 3`UTR and adjacent coding regions, and the modulation of these interactions by lovastatin, strongly suggest a role in the post-transcriptional regulation of RNA stability. These data provided a basis for future studies on the mechanisms of regulation of transcripts stability, and suggest potential molecular targets for the manipulation of eNOS expression in endothelial cells.

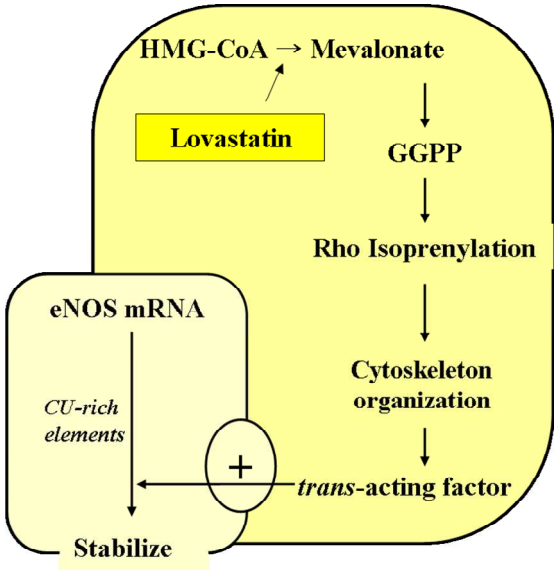

Fig. 19. Mechanisms responsible for the regulation of eNOS mRNA stability by lovastatin

Ⅴ References

1. Moncada, S. and A. Higgs, *The L-arginine-nitric oxide pathway.* N Engl J M ed, 1993. **329**(27): p. 2002-12.
2. Sessa, W.C., *The nitric oxide synthase family of proteins.* J Vasc Res, 1994. **31**(3): p. 131-43.
3. Griffith, T.M., et al., *EDRF coordinates the behaviour of vascular resistance vessels.* Nature, 1987. **329**(6138): p. 442-5.
4. Furchgott, R.F. and P.M. Vanhoutte, *Endothelium-derived relaxing and contra cting factors.* Faseb J, 1989. **3**(9): p. 2007-18.
5. Moncada, S., R.M. Palmer, and E.A. Higgs, *Nitric oxide: physiology, pathophy siology, and pharmacology.* Pharmacol Rev, 1991. **43**(2): p. 109-42.
6. Forstermann, U., J.P. Boissel, and H. Kleinert, *Expressional control of the 'c onstitutive' isoforms of nitric oxide synthase (NOS I and NOS III).* Faseb J, 1 998. **12**(10): p. 773-90.
7. Le Cras, T.D., et al., *Chronic hypoxia upregulates endothelial and inducible NO synthase gene and protein expression in rat lung.* Am J Physiol, 1996. **2 70**(1 Pt 1): p. L164-70.
8. Lopez-Farre, A., et al., *Role of nitric oxide in autocrine control of growth an d apoptosis of endothelial cells.* Am J Physiol, 1997. **272**(2 Pt 2): p. H760-8.
9. Mohamed F, M.J., Gordon A, Cernacek P, Blais D, Stewart DJ., *Lack of role for nitric oxide (NO) in the selective destabilization of endothelial NO syntha se mRNA by tumor necrosis factor-alpha.* Arterioscler Thromb Vasc Biol. , 1 995. **15**(1): p. 52-7.
10. Yoshizumi, M., et al., *Tumor necrosis factor downregulates an endothelial nit ric oxide synthase mRNA by shortening its half-life.* Circ Res, 1993. **73**(1): p. 205-9.
11. Venema, R.C., et al., *Organization of the bovine gene encoding the endotheli al nitric oxide synthase.* Biochim Biophys Acta, 1994. **1218**(3): p. 413-20.
12. Marsden, P.A., et al., *Structure and chromosomal localization of the human c onstitutive endothelial nitric oxide synthase gene.* J Biol Chem, 1993. **268**(23): p. 17478-88.
13. Zhang, R., W. Min, and W.C. Sessa, *Functional analysis of the human endothe lial nitric oxide synthase promoter. Sp1 and GATA factors are necessary for basal transcription in endothelial cells.* J Biol Chem, 1995. **270**(25): p. 1532 0-6.
14. Karantzoulis-Fegaras, F., et al., *Characterization of the human endothelial nit ric-oxide synthase promoter.* J Biol Chem, 1999. **274**(5): p. 3076-93.
15. Chan, Y., et al., *The cell-specific expression of endothelial nitric-oxide synt hase: a role for DNA methylation.* J Biol Chem, 2004. **279**(33): p. 35087-10 0.

16. Nguyen, C.T., F.A. Gonzales, and P.A. Jones, *Altered chromatin structure ass ociated with methylation-induced gene silencing in cancer cells: correlation o f accessibility, methylation, MeCP2 binding and acetylation.* Nucleic Acids Re s, 2001. **29**(22): p. 4598-606.
17. Robertson, K.D. and A.P. Wolffe, *DNA methylation in health and disease.* Nat Rev Genet, 2000. **1**(1): p. 11-9.
18. Schubeler, D., et al., *Genomic targeting of methylated DNA: influence of met hylation on transcription, replication, chromatin structure, and histone acetyla tion.* Mol Cell Biol, 2000. **20**(24): p. 9103-12.
19. Laufs, U., V.L. Fata, and J.K. Liao, *Inhibition of 3-hydroxy-3-methylglutaryl (HMG)-CoA reductase blocks hypoxia-mediated down-regulation of endotheli al nitric oxide synthase.* J Biol Chem, 1997. **272**(50): p. 31725-9.
20. Bouloumie, A., V.B. Schini-Kerth, and R. Busse, *Vascular endothelial growth factor up-regulates nitric oxide synthase expression in endothelial cells.* Car diovasc Res, 1999. **41**(3): p. 773-80.
21. Jacobson, A. and S.W. Peltz, *Interrelationships of the pathways of mRNA dec ay and translation in eukaryotic cells.* Annu Rev Biochem, 1996. **65**: p. 693-739.
22. Hentze, M.W. and L.C. Kuhn, *Molecular control of vertebrate iron metabolism: mRNA-based regulatory circuits operated by iron, nitric oxide, and oxidativ e stress.* Proc Natl Acad Sci U S A, 1996. **93**(16): p. 8175-82.
23. Searles, C.D., et al., *Posttranscriptional regulation of endothelial nitric oxide synthase during cell growth.* Circ Res, 1999. **85**(7): p. 588-95.
24. Alonso, J., et al., *Endothelial cytosolic proteins bind to the 3' untranslated re gion of endothelial nitric oxide synthase mRNA: regulation by tumor necrosis factor alpha.* Mol Cell Biol, 1997. **17**(10): p. 5719-26.
25. Rus, H.G., F. Niculescu, and R. Vlaicu, *Tumor necrosis factor-alpha in human arterial wall with atherosclerosis.* Atherosclerosis, 1991. **89**(2-3): p. 247-54.
26. Gonzalez-Fernandez, F., et al., *Cerivastatin prevents tumor necrosis factor-al pha-induced downregulation of endothelial nitric oxide synthase: role of endo thelial cytosolic proteins.* Atherosclerosis, 2001. **155**(1): p. 61-70.
27. Sanchez de Miguel, L., et al., *Evidence that an endothelial cytosolic protein binds to the 3'-untranslated region of endothelial nitric oxide synthase mRN A.* J Vasc Res, 1999. **36**(3): p. 201-8.
28. Lai, P.F., et al., *Downregulation of eNOS mRNA expression by TNFalpha: ide ntification and functional characterization of RNA-protein interactions in the 3'UTR.* Cardiovasc Res, 2003. **59**(1): p. 160-8.
29. Laufs, U., et al., *Upregulation of endothelial nitric oxide synthase by HMG C oA reductase inhibitors.* Circulation, 1998. **97**(12): p. 1129-35.
30. Kano, H., et al., *A HMG-CoA reductase inhibitor improved regression of ath erosclerosis in the rabbit aorta without affecting serum lipid levels: possible*

relevance of up-regulation of endothelial NO synthase mRNA. Biochem Biophys Res Commun, 1999. **259**(2): p. 414-9.

31. Ozaki, K., et al., *Regulation of endothelial nitric oxide synthase and endothelin-1 expression by fluvastatin in human vascular endothelial cells.* Jpn J Pharmacol, 2001. **85**(2): p. 147-54.
32. Shepherd, J., et al., *Prevention of coronary heart disease with pravastatin in men with hypercholesterolemia. West of Scotland Coronary Prevention Study Group.* N Engl J Med, 1995. **333**(20): p. 1301-7.
33. *Randomised trial of cholesterol lowering in 4444 patients with coronary heart disease: the Scandinavian Simvastatin Survival Study (4S).* Lancet, 1994. **344**(8934): p. 1383-9.
34. Maron, D.J., S. Fazio, and M.F. Linton, *Current perspectives on statins.* Circulation, 2000. **101**(2): p. 207-13.
35. *Influence of pravastatin and plasma lipids on clinical events in the West of Scotland Coronary Prevention Study (WOSCOPS).* Circulation, 1998. **97**(15): p. 1440-5.
36. Lefer, A.M., et al., *Simvastatin preserves the ischemic-reperfused myocardium in normocholesterolemic rat hearts.* Circulation, 1999. **100**(2): p. 178-84.
37. Rikitake, Y. and J.K. Liao, *Rho GTPases, statins, and nitric oxide.* Circ Res, 2005. **97**(12): p. 1232-5.
38. Chomczynski, P. and N. Sacchi, *Single-step method of RNA isolation by acid guanidinium thiocyanate-phenol-chloroform extraction.* Anal Biochem, 1987. **162**(1): p. 156-9.
39. Wang, X., et al., *Detection and characterization of a 3' untranslated region ribonucleoprotein complex associated with human alpha-globin mRNA stability.* Mol Cell Biol, 1995. **15**(3): p. 1769-77.
40. Ke, S.H. and E.L. Madison, *Rapid and efficient site-directed mutagenesis by single-tube 'megaprimer' PCR method.* Nucleic Acids Res, 1997. **25**(16): p. 3371-2.
41. Mukudai, Y., et al., *Regulation of chicken ccn2 gene by interaction between RNA cis-element and putative trans-factor during differentiation of chondrocytes.* J Biol Chem, 2005. **280**(5): p. 3166-77.
42. Kubota, S., et al., *Identification of an RNA element that confers post-transcriptional repression of connective tissue growth factor/hypertrophic chondrocyte specific 24 (ctgf/hcs24) gene: similarities to retroviral RNA-protein interactions.* Oncogene, 2000. **19**(41): p. 4773-86.
43. de Moor, C.H., et al., *Proteins binding to the leader of the 6.0 kb mRNA of human insulin-like growth factor 2 influence translation.* Biochem J, 1995. **307 (Pt 1)**: p. 225-31.
44. McCormac, D.J., et al., *Light-associated and processing-dependent protein binding to 5' regions of rbcL mRNA in the chloroplasts of a C4 plant.* J Biol Chem, 2001. **276**(5): p. 3476-83.

45. Garige, M., M. Gong, and M.R. Lakshman, *Ethanol destabilizes liver Gal beta 1, 4GlcNAc alpha2,6-sialyltransferase, mRNA by depleting a 3'-untranslated region-specific binding protein.* J Pharmacol Exp Ther, 2006. **318**(3): p. 1076-82.
46. Laufs, U., et al., *Neuroprotection mediated by changes in the endothelial actin cytoskeleton.* J Clin Invest, 2000. **106**(1): p. 15-24.
47. Van Aelst, L. and C. D'Souza-Schorey, *Rho GTPases and signaling networks.* Genes Dev, 1997. **11**(18): p. 2295-322.
48. Hall, A., *Rho GTPases and the actin cytoskeleton.* Science, 1998. **279**(5350): p. 509-14.
49. Laufs, U. and J.K. Liao, *Post-transcriptional regulation of endothelial nitric oxide synthase mRNA stability by Rho GTPase.* J Biol Chem, 1998. **273**(37): p. 24266-71.
50. Eto, M., et al., *Thrombin suppresses endothelial nitric oxide synthase and up regulates endothelin-converting enzyme-1 expression by distinct pathways: role of Rho/ROCK and mitogen-activated protein kinase.* Circ Res, 2001. **89**(7): p. 583-90.
51. Takemoto, M., et al., *Rho-kinase mediates hypoxia-induced downregulation of endothelial nitric oxide synthase.* Circulation, 2002. **106**(1): p. 57-62.
52. Arriero, M.M., et al., *Aspirin prevents Escherichia coli lipopolysaccharide- and Staphylococcus aureus-induced downregulation of endothelial nitric oxide synthase expression in guinea pig pericardial tissue.* Circ Res, 2002. **90**(6): p. 719-27.
53. Jimenez, A., et al., *Regulation of endothelial nitric oxide synthase expression in the vascular wall and in mononuclear cells from hypercholesterolemic rabbits.* Circulation, 2001. **104**(15): p. 1822-30.
54. Nagy, E. and W.F. Rigby, *Glyceraldehyde-3-phosphate dehydrogenase selectively binds AU-rich RNA in the NAD(+)-binding region (Rossmann fold).* J Biol Chem, 1995. **270**(6): p. 2755-63.
55. Kaptain, S., et al., *A regulated RNA binding protein also possesses aconitase activity.* Proc Natl Acad Sci U S A, 1991. **88**(22): p. 10109-13.
56. Scandurro, A.B., et al., *Interaction of erythropoietin RNA binding protein with erythropoietin RNA requires an association with heat shock protein 70.* Kidney Int, 1997. **51**(2): p. 579-84.
57. Hirata, K., et al., *Low concentration of oxidized low-density lipoprotein and lysophosphatidylcholine upregulate constitutive nitric oxide synthase mRNA expression in bovine aortic endothelial cells.* Circ Res, 1995. **76**(6): p. 958-62.
58. McQuillan, L.P., et al., *Hypoxia inhibits expression of eNOS via transcriptional and posttranscriptional mechanisms.* Am J Physiol, 1994. **267**(5 Pt 2): p. H1921-7.
59. Liao, J.K., et al., *Oxidized low-density lipoprotein decreases the expression of endothelial nitric oxide synthase.* J Biol Chem, 1995. **270**(1): p. 319-24.

60. Searles, C.D., et al., *Actin cytoskeleton organization and posttranscriptional r egulation of endothelial nitric oxide synthase during cell growth.* Circ Res, 2004. **95**(5): p. 488-95.
61. Weber, M., et al., *Laminar shear stress and 3' polyadenylation of eNOS mRNA.* Circ Res, 2005. **96**(11): p. 1161-8.

Ⅵ Abstract in Korean

Sterol-반응성 인자에 의한 인간내피세포의 nitric oxide synthase mRNA 안정성의 조절

송국화
연세대학교 대학원 의학과

Statin계 약물은 cholesterol 생합성 과정에서 mevalonate 합성 경로의 속도-조절 효소를 억제하므로서 혈중 cholesterol 치를 낮춘다. 따라서, 이 약물들은 심 혈관계 질환 환자 및 이 질병에 걸릴 위험이 큰 사람들에게 흔히 사용된다. 최근들어서, statin계 약물들이 cholesterol 치를 낮추는 것 외에도 다른 작용을 통해서 죽상 경화증을 예방할 수 있음이 보고되고 있다.

본 연구진은 HUVEC에서 유래된 세포주인 EA.hy926을 이용한 실험에서 lovastatin이 eNOS mRNA 치를 증가시킴을 보고한 바 있다. Lovastatin은 mevalonate 및 geranylgeranyl pyrophosphate (GGPP)와 같은 sterol을 세포 내에서 고갈시키므로서 eNOS mRNA을 안정화시켰다. GGPP는 다양한 세포내 신호 전달 단백의 isoprenylation에 필요하므로, lovastatin은 특정한 신호 전달 과정을 억제하므로서 이러한 효과를 나타낸 것으로 생각되었다. 또한, 이 실험에서 eNOS mRNA의 제거율을 조절하는 cis-acting element들이 3'-UTR 및 이에 인접한 부위에 있음이 관찰되었다. 추후 실험에서, Rho-kinase 억제제인 hydroxyfasudil 및 actin cytoskeleton 파괴 물질인 cytochalasin D가 eNOS mRNA 치를 증가시킴이 관찰되므로서, Rho 신호 전달 경로에 의해 조절되는 세포 구조의 상태가 eNOS mRNA의 제거율에 영향을 미칠 수 있음이 제시된 바 있다.

본 실험에서는 eNOS mRNA의 안정성을 조절하는 cis-acting element들의 염기 서열과 정확한 위치를 결정하고자 하였다. CU-rich element에 대응하는 mutant들을 이용한 transfection 실험에서 UCCUC, UUCUC, CUUU, UCCUU, CCUCC, CCUCU가 eNOS mRNA 안정성 조절에 관여함이 관찰되었다. 이들 cis-acting element와 결합하는 trans-acting

factor가 존재함을 확인하기 위하여 동위 원소로 표지된 RNA probe과 세포 추출물을 이용하여 RNA-단백 반응 실험을 시행하였다. 이 실험에서 60 kDa riboprobe-단백 복합체가 관찰되었고, lovastatin으로 세포를 전처치하였을 때, 이 riboprobe-단백 복합체의 형성이 증가됨이 확인되었다. 이 단백을 biotin-표지 RNA probe을 이용하여 분리한 후 이차원 겔 전기영동을 시행하였고, Maldi-TOF spectrum 분석에서 이 단백이 β-actin임이 제시되었다. 이상의 실험 결과는 세포내 sterol이 고갈되었을 때, β-actin이 sterol-responsive element (CU-rich element)에 결합하므로서 eNOS mRNA의 안정성을 증가시킴을 제시하고 있다.

Key words: statin, eNOS mRNA 안정성, CU-rich element, 60 kD ribonucleoprotein, β-actin